

Environmental Monitoring Program

Contents

I General	5
1 Program Information	7
1.1 Videos	8
II Annual Reports	9
2 Continuous Water Quality	11
2.1 Background	11
2.2 Current Report	11
2.3 Contact Info	34
3 Discrete Water Quality	35
3.1 Current Report	36
3.2 Data and Archived Reports	43
4 Benthic Invertebrates	47
4.1 Metadata	48
4.2 Current Report	51
4.3 Data and Archived Reports	60
5 Phytoplankton	61
5.1 Current Report	63
5.2 Contact Info	77

6	Zooplankton	79
6.1	Current Report	81
6.2	Data and Contact Info	91
III	Special Studies	93
7	Coming Soon!	95

Part I

General

Chapter 1

Program Information

THIS IS A TEST SITE. For official annual EMP reports, please contact Sarah Perry at sarah.perry@water.ca.gov.

The State Water Resources Control Board (SWRCB) sets water quality objectives to protect beneficial uses of water in the Sacramento-San Joaquin Delta and Suisun and San Pablo Bays. These objectives are met by establishing standards mandated in water right permits issued to the Department of Water Resources and U.S. Bureau of Reclamation by the SWRCB. The standards include minimum Delta outflows, limits to Delta water export by the State Water Project (SWP) and the Central Valley Project (CVP), and maximum allowable salinity levels.

In 1971, the State Water Resources Control Board (SWRCB) established Water Right Decision 1379 (D-1379). This Decision contained new water quality requirements for the San Francisco Bay-Delta Estuary. D-1379 was also the first water right decision to provide terms and conditions for a comprehensive monitoring program to routinely determine water quality conditions and changes in environmental conditions within the estuary. The monitoring program described in D-1379 was developed by the Stanford Research Institute through a contract with the SWRCB. Implementation of the monitoring program began in 1972, as SWRCB, DWR, and USBR met to define their individual responsibilities for various elements of the monitoring program. In 1978, amendments to water quality standards were implemented and resulted in Water Right Decision 1485 (D-1485). These standards were again amended under the 1995 Water Quality Control Plan and Water Right Decision 1641 (D-1641) established in 1999. The SWP and CVP are currently operated to comply with the monitoring and reporting requirements described in D-1641. D-1641 requires DWR and USBR to conduct a comprehensive environmental monitoring program to determine compliance with the water quality standards and also to submit an annual report to the SWRCB discussing data collected.

More information about EMP and its connection to the Interagency Ecological Program (IEP) can be found here. To watch EMP in action, click here for discrete monitoring and here for continuous monitoring.

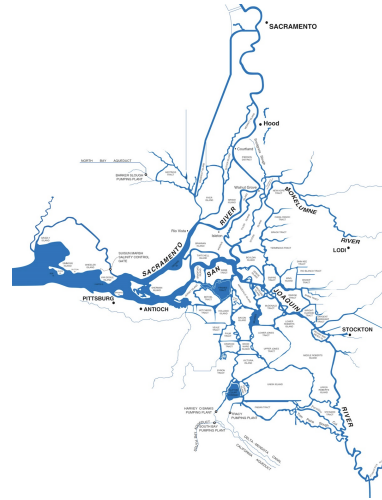


Figure 1.1: Map of the Sacramento-San Joaquin Delta. Source: DWR

1.1 Videos

Part II

Annual Reports

Chapter 2

Continuous Water Quality

2.1 Background

The Continuous Environmental Monitoring Program (CEMP) provides real-time quarter-hourly water quality and environmental data from 15 automated sampling stations in the estuary (Figure 1). The stations provide continuous measurements of 6 water quality parameters and up to 4 environmental parameters at select locations. These measurements are used by operators of the State Water Project (SWP) and the Central Valley Project (CVP) to assess the impacts of the project operations and to adjust project operations to comply with mandated water quality standards. The continuous monitoring program has been in operation since 1983. This report summarizes the results of continuous water quality monitoring at 15 sites for calendar year 2020. The stations are categorized into 5 regions. (Table 1, Figure 2): Northern Interior Delta, Southern Interior Delta, Central Delta, Confluence and Grizzly & Suisun Bays.

NOTE: CEMP's Sherman Island station (SSI), which was called D11A in previous reports, has been renamed D22A to better reflect it's location in relation to historical station D22.

2.2 Current Report

2.2.1 Methods

Continuous data were collected for the water quality and environmental parameters shown in Table 2. Each of the 15 monitoring stations collected continuous data for water temperature (WT), pH, dissolved oxygen (DO), surface specific conductance (SpC), chlorophyll a fluorescence, and turbidity. Additional sensors were installed at the Antioch, Mallard Island, and Martinez stations in

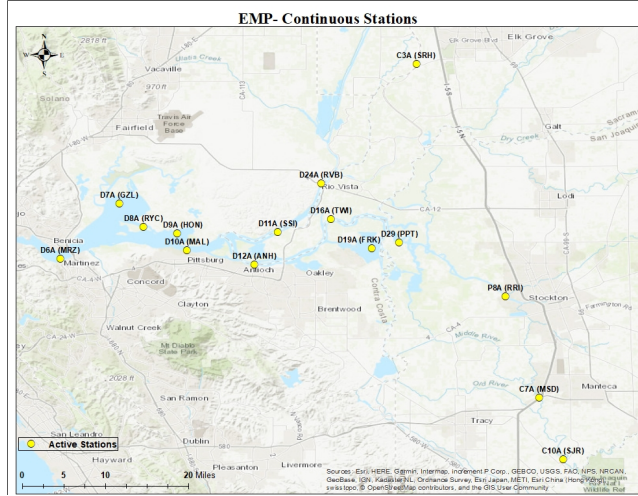


Figure 2.1: Map of EMP Continuous Water Quality Stations.

Table 2.1: Regions of Continuous EMP

Region	Stations
Northern Interior Delta	C3A (Hood), D24A (Rio Vista)
Central Delta	D16A (Twitchell Island), D19A (Franks Tract)
Southern Interior Delta	P8A (Stockton), C7A (Mossdale), C10A (SJR)
Confluence	D22A (Sherman Island), D12A (Antioch), D11A (SSB)
Grizzly and Suisun Bay	D9A (Honker Bay), D8A (Ryer Island), D7A (Grizzly Bay)

Table 2.2: Parameters sampled by Continuous EMP

Parameter	Units	Frequency
Water Temperature	deg-C	15 minute instantaneous
Specific Conductance	uS/cm	15 minute instantaneous
DO	mg/L	15 minute instantaneous
pH	unitless	15 minute instantaneous
Turbidity	NTU	15 minute instantaneous
Fluorescence	FU	15 minute instantaneous

the 1990's to monitor bottom SpC. These measurements, along with river stage data measured at the Mallard Island and Martinez stations, were needed to determine compliance with the salinity standard (also known as X2) that was mandated by the Bay-Delta Plan (SWRCB, 1995).

Environmental data, such as air temperature (AT), solar radiation (SRI), wind speed (WV), and wind direction (WD), were measured at all stations as part of D-1641's objectives (SWRCB, 1999). The only environmental parameter analyzed for this report was air temperature from a MET-1 Instrument Mod. 062 sensor.

Except for bottom specific conductance, all water samples were collected at 1-m below the water surface using a float-mounted YSI EXO2 multi-parameter water quality sonde. In contrast, bottom specific conductance was measured at 1.5 m above the channel bottom using a YSI EXO1 sonde. Water quality data and environmental data were recorded at 15-minute intervals.

2.2.2 QA Status

On a monthly basis, quality assurance and control measures were applied using field verification data sheets. Data that did not pass quality control checks or were affiliated with instrument issues were flagged and excluded from the analysis.

2.2.3 Regions

The daily averages of the continuous 15-minute data collected for air and water temperature, pH, DO, surface and bottom SpC, chlorophyll a fluorescence, and

Table 2.3: Rating criteria for continuous sonde calibration

Analyte	Excellent	Good
Water Temperature (deg-C)	<±0.2	±0.2-0.5
Specific Conductance (uS/cm)	<±3%	±3-10%
Dissolved Oxygen (mg/L)	<±0.3 or <±5%	±0.3-0.5 or or ±5-10%
pH	<±0.2	±0.2-0.5
Turbidity (NTU)	<±0.5 or <±5%	±0.5-1.0 or ±5-10%

turbidity for calendar year 2020 are shown in Figures 4 to 8. The range of monthly DO values at the Stockton station is shown below.

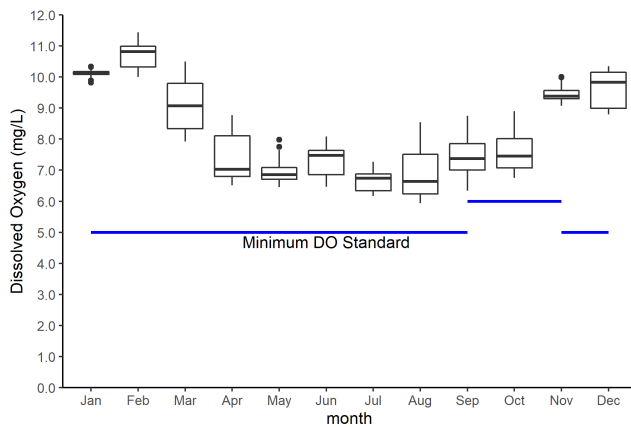


Figure 2.2: Range of daily dissolved oxygen Rough and Ready Isl. (P8), 2020

2.2.3.1 Northern Interior Delta

The Northern Interior Delta stations had surface specific conductance values that ranged from 125 uS/cm (C3A in July) to 541 uS/cm (D24A in November). Surface turbidity values ranged from 1.7 NTU (C3A in October) to 41.27 NTU (C3A in January). Surface water temperature values ranged from 8.57 °C (C3A in January) to 25.44 °C (D24A in August). Surface dissolved oxygen values ranged from 6.67 mg/L (D24A in August) to 11.19 mg/L (C3A in January). Surface pH values ranged from 7.12 (C3A in May) to 7.86 (D24A in March). Surface fluorescence values ranged from 0.12 ug/L (D24A in November) to 10.90 ug/L (C3A in April).

Table 2.4: Summary statistics for Northern Interior Delta, 2020

Statistic	Specific Conductance (us/cm)	Turbidity (NTU)	Water Temperature
	Surface	Surface	Surface
MIN	125	1.71	8.57
MAX	541	41.27	25.44
AVERAGE	188	5.24	17.04

Table 2.5: Summary statistics for Central Interior Delta, 2020

Statistic	Specific Conductance (us/cm)	Turbidity (NTU)	Water Temperature
	Surface	Surface	Surface
MIN	172	0.28	8.64
MAX	1484	77.16	26.95
AVERAGE	463	3.68	17.5

2.2.3.2 Central Interior Delta

The Central Interior Delta stations had surface specific conductance values that ranged from 172 uS/cm (D29 in July) to 1484 uS/cm (D16A in August). Surface turbidity values ranged from 0.28 NTU (D19A in October) to 77.16 NTU (D19A in February). Surface water temperature values ranged from 8.64 °C (D19A in January) to 26.95 °C (D19A in August). Surface dissolved oxygen values ranged from 6.97 mg/L (D29 in August) to 13.69 mg/L (D19A in August). Surface pH values ranged from 7.40 (D29 in February to 9.64 (D19A in June). Surface fluorescence values ranged from 0.55 ug/L (D19A in August) to 19.32 ug/L (D29 in August).

2.2.3.3 Southern Interior Delta

The Southern Interior Delta stations had surface specific conductance values that ranged from 177 uS/cm (C10A in July) to 995 uS/cm (P8A in December). Surface turbidity values ranged from 1.20 NTU (P8A in November) to 57.83 NTU (C10A in April). Surface water temperature values ranged from 8.65 °C (C10A in December) to 29.56 °C (C7A in August). Surface dissolved oxygen values ranged from 5.94 mg/L (P8A in August) to 15.06 mg/L (C10A in July). Surface pH values ranged from 7.3 (P8A in May) to 9.18 (C7A in July). Surface fluorescence values ranged from 0.73 ug/L (P8A in June) to 72.76 ug/L (C10A in July).

Table 2.6: Summary statistics for Southern Interior Delta, 2020

Statistic	Specific Conductance (us/cm)	Turbidity (NTU)	Water Temp
	Surface	Surface	
MIN	177	1.2	
MAX	995	57.83	
AVERAGE	553	7.3	

Table 2.7: Rating criteria for Confluence, 2020

Statistic	Specific Conductance (s/cm)	Specific Conductance (us/cm)	
	Surface	Bottom	
MIN	209	410	
MAX	16086	16819	
AVERAGE	4382	6102	

2.2.3.4 Confluence

The Confluence stations had surface specific conductance values that ranged from 209 uS/cm (D22A in February) to 16,086 uS/cm (D10A in November). Bottom specific conductance values ranged from 410 uS/cm (D12A in April) to 16818 uS/cm (D10A in December). Surface turbidity values ranged from 3.56 NTU (D12A in October) to 95.4 NTU (D22A in December). Surface water temperature values ranged from 9.0 2 °C (D12A in January) to 24.42 °C (D22A in August). Bottom water temperature values ranged from 9.03 °C (D12A in January) to 24.24 °C (D12A in August). Surface dissolved oxygen values ranged from 7.56 mg/L (D22A in August) to 10.95 mg/L (D12A in February). Surface pH values ranged from 7.52 (D22A in February) to 8.07 (D12A in August). Surface fluorescence values ranged from 0.65 ug/L (D10A in April) to 6.87 ug/L (D22A in October).

2.2.3.5 Grizzly/Suisun Bay

The Grizzly Suisun Bay stations had surface specific conductance values that ranged from 2,026 uS/cm (D9A in June) to 30,939 uS/cm (D6A in November). Bottom specific conductance values ranged from 2,026 uS/cm (D10A in January) to 33,350 uS/cm (D6A in November). Surface turbidity values ranged from 5.0 NTU (D6A in September) to 98.8 NTU (D7A in March). Surface water temperature values ranged from 8.97 °C (D9A in February) to 23.61 °C (D10A in November).

Table 2.8: Rating criteria for Grizzly/Suisun Bay, 2020

Statistic	Specific Conductance (us/cm)	Specific Conductance (us/cm)_1	Tur
	Surface	Bottom	
MIN	1933	2026	
MAX	30939	33350	
AVERAGE	13913	18080	

in August). Bottom water temperature values ranged from 9.11 °C (D10A in January) to 23.57 °C (D10A in August). Surface dissolved oxygen values ranged from 7.21 mg/L (D6A in August) to 10.6 mg/L (D9A in January). Surface pH values ranged from 7.54 (D9A in January) to 8.19 (D8A in May). Surface fluorescence values ranged from 0.62 ug/L (D9A in December) to 9.32 ug /L (D7A in November).

2.2.4 Parameters

2.2.4.1 Water Temperature

Average daily water temperatures in the estuary ranged from 8.57 °C to 29.6°C, with the lower values in the Northern Interior Delta location and the higher values found in the Southern Interior Delta stations. Average daily water temperatures at the Northern Interior Delta stations were usually lower in comparison to the Southern Interior Delta stations, with the greatest divergence occurring in the months of July through September at the Southern Interior Delta locations.

2.2.4.2 Specific Conductance

Daily average surface specific conductance for the estuary ranged from 125 uS/cm to 30,939 uS/cm, with the lower values in the Northern Interior Delta stations and the higher values at the more tidally influenced Grizzly/Suisun Bay locations (Figure 3e).

The Central Delta Stations showed increases in specific conductance from August onward (Figure 3c). In addition, the Southern Interior Delta stations on the San Joaquin River showed a large decrease in surface specific conductance in October through November (Figure 3b).

Bottom specific conductance measured in 2020 at D12A, D10A, and D6A stations exhibited seasonal patterns and ranges similar to the surface specific conductance (Figure 3f).



Figure 2.3: Average daily water temperature in the Northern Interior Delta, 2020



Figure 2.4: Average daily water temperature in the Southern Interior Delta, 2020

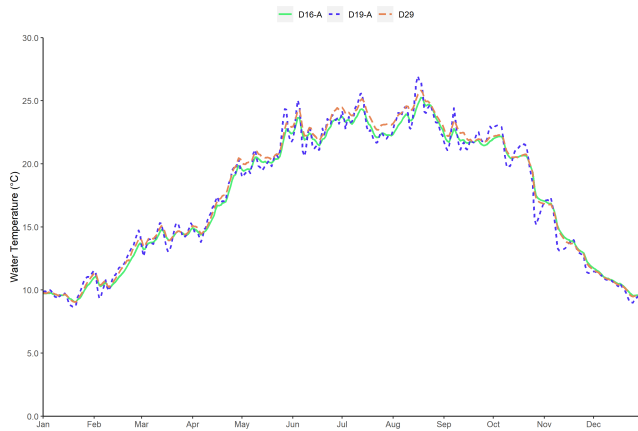


Figure 2.5: Average daily water temperature in the Central Delta, 2020



Figure 2.6: Average daily water temperature in the Confluence, 2020



Figure 2.7: Average daily water temperature in the Grizzly/Suisun Bays, 2020



Figure 2.8: Average daily specific conductance in the Northern Interior Delta, 2020

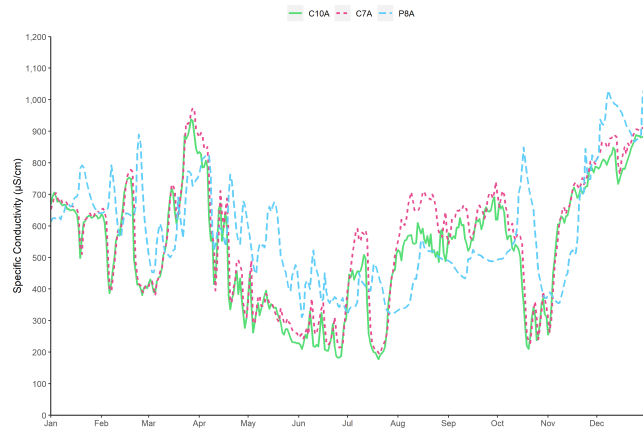


Figure 2.9: Average daily specific conductance in the Southern Interior Delta, 2020



Figure 2.10: Average daily specific conductance in the Central Delta, 2020

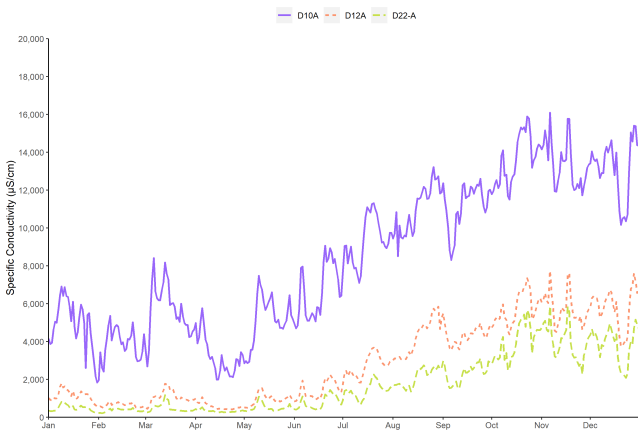


Figure 2.11: Average daily specific conductance in the Confluence, 2020

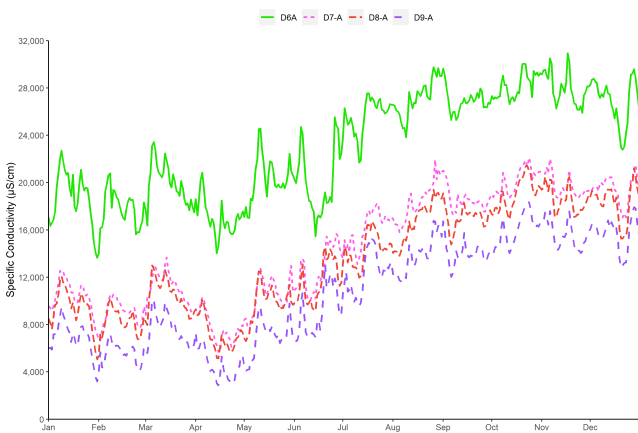


Figure 2.12: Average daily specific conductance in the Grizzly/Suisun Bays, 2020

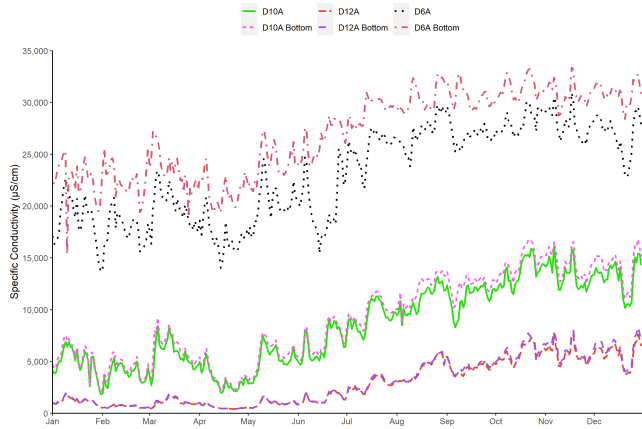


Figure 2.13: Average daily specific conductance Surface-Bottom, 2020

2.2.4.3 Dissolved Oxygen

Average daily DO values in the estuary ranged from 5.94 mg/L to 15.1 mg/L (Figure 4a to 4e). The greatest degree of variability was seen at the Southern Interior Delta stations.

All compliance monitoring stations recorded daily averages above the standard of 5.0 mg/L that was set by the CVRWQCB in the Basin Plan (CVRWQCB, 1998). The monthly average DO levels at the Stockton station did not fall below the 5.0 mg/L standard that was set by the CVRWQCB (1998). The monthly average DO levels did not drop below the 6.0 mg/L standard (SWRCB, 1995) for the passage of fall-run Chinook salmon through the ship channel for the September through November 2020 control period.

2.2.4.4 pH

Daily average pH levels at all stations in the estuary ranged from 7.12 to 9.64 (Figure 5a to 5e). The Southern Interior Delta stations showed a large increase in daily average pH beginning June 2020 to September 2020 (Figure 5b). The Central Delta station D19A showed an increase in pH values beginning April 2020 until the end of October 2020 (Figure 5c).

2.2.4.5 Turbidity

Daily average turbidity levels at all stations in the estuary ranged from 0.28 to 98.8 (Figure 6a to 6e). The Northern Interior Delta stations showed a large increase in turbidity in January and February, peaking at 41.27 FNU (Figure 6a).



Figure 2.14: Average daily dissolved oxygen in the Northern Interior Delta, 2020



Figure 2.15: Average daily dissolved oxygen in the Southern Interior Delta, 2020

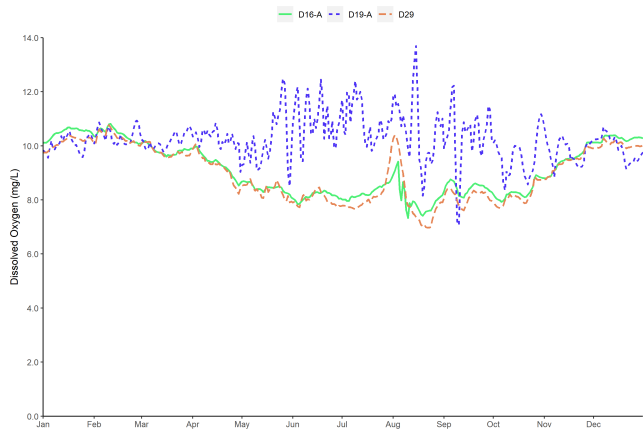


Figure 2.16: Average daily dissolved oxygen in the Central Delta, 2020



Figure 2.17: Average daily dissolved oxygen in the Confluence, 2020



Figure 2.18: Average daily dissolved oxygen in the Grizzly/Suisun Bays, 2020

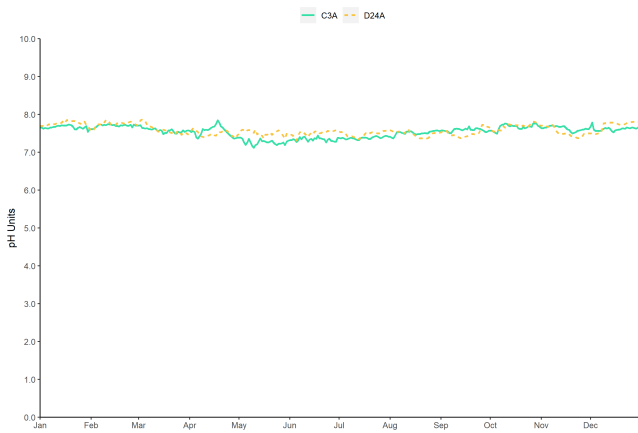


Figure 2.19: Average daily pH in the Northern Interior Delta, 2020

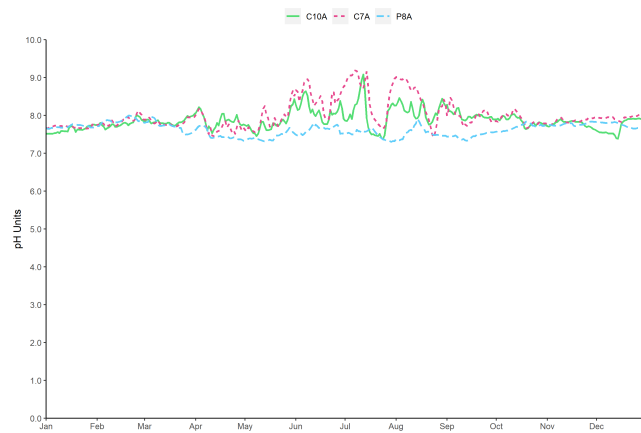


Figure 2.20: Average daily pH in the Southern Interior Delta, 2020



Figure 2.21: Average daily pH in the Central Delta, 2020



Figure 2.22: Average daily pH in the Confluence, 2020

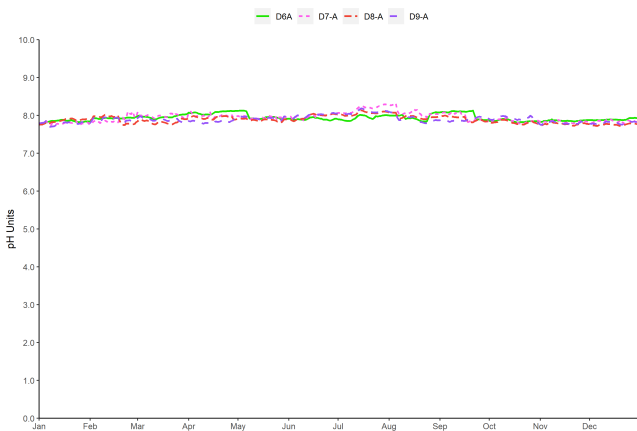


Figure 2.23: Average daily pH in the Grizzly/Suisun Bays, 2020

The Southern interior Delta stations all showed a significant spike in turbidity readings in mid-April which gradually decreased through May (figure 6b).

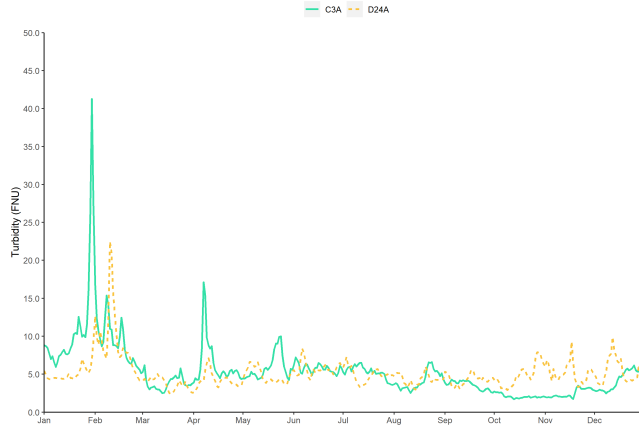


Figure 2.24: Average daily turbidity in the Northern Interior Delta, 2020

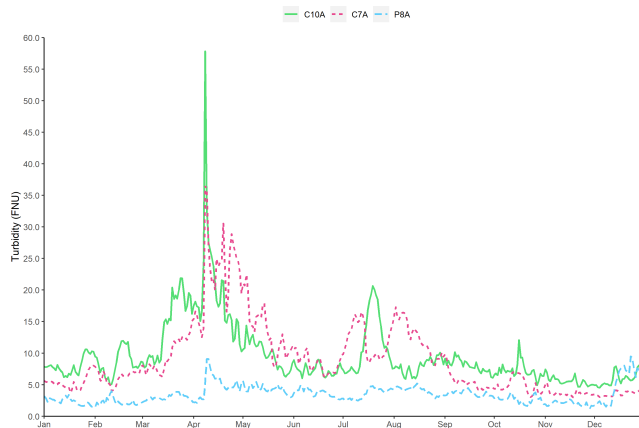


Figure 2.25: Average daily turbidity in the Southern Interior Delta, 2020

2.2.4.6 Chlorophyll a Fluorescence

Daily average chlorophyll a fluorescence recorded at all the stations ranged from a low of 0.12 ($\mu\text{g/L}$) in December 2020 for the Northern Interior station D24A to a high of 72.8 ($\mu\text{g/L}$) in July 2020 for the Southern Interior Delta station C10A (Figure 7a to 7e).

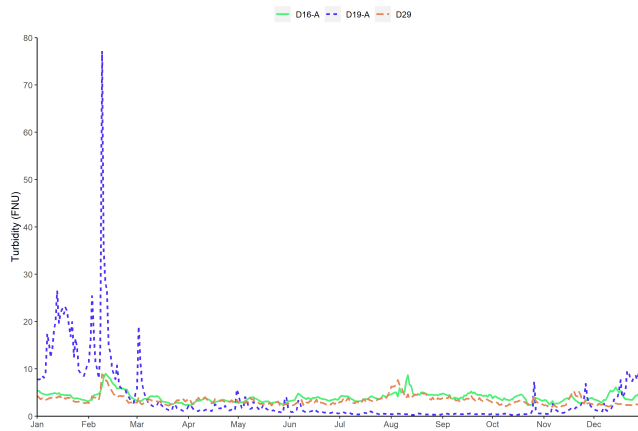


Figure 2.26: Average daily turbidity in the Central Delta, 2020

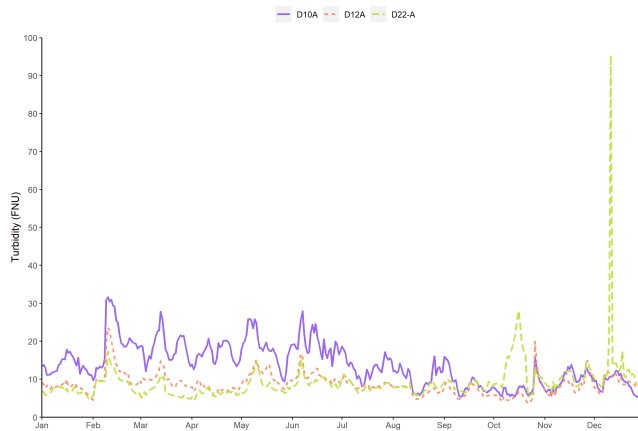


Figure 2.27: Average daily turbidity in the Confluence, 2020

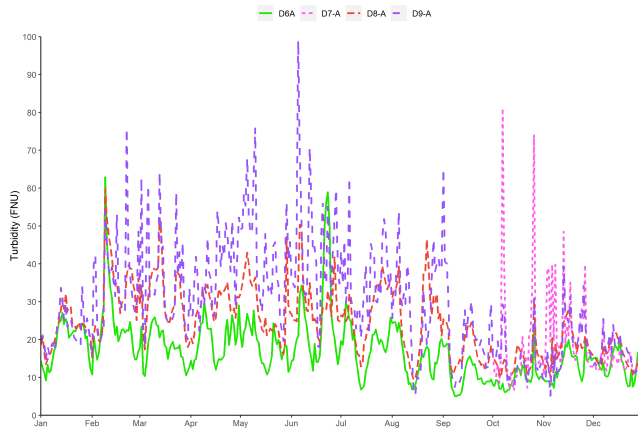


Figure 2.28: Average daily turbidity in the Grizzly/Suisun Bays, 2020

For most of the 2020 calendar year, daily fluorescence averages at Southern Interior Delta stations were higher than other regions with sustained higher values, with the exception of P8A (Figure 7b).

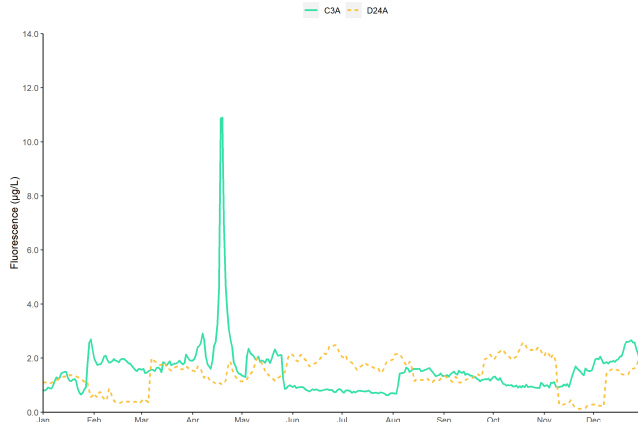


Figure 2.29: Average daily fluorescence in the Northern Interior Delta, 2020

2.2.4.7 Air Temperature

Daily average air temperatures in the estuary ranged from 3.38°C in December 2020 at Northern Interior station C3A to 33.27°C in August 2020 at the Southern Interior Delta station C7A.

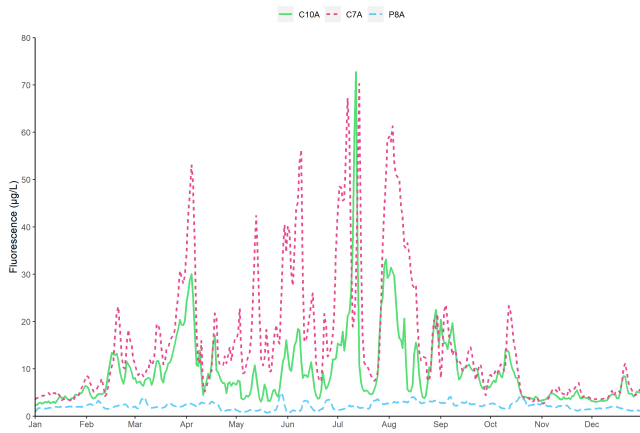


Figure 2.30: Average daily fluorescence in the Southern Interior Delta, 2020

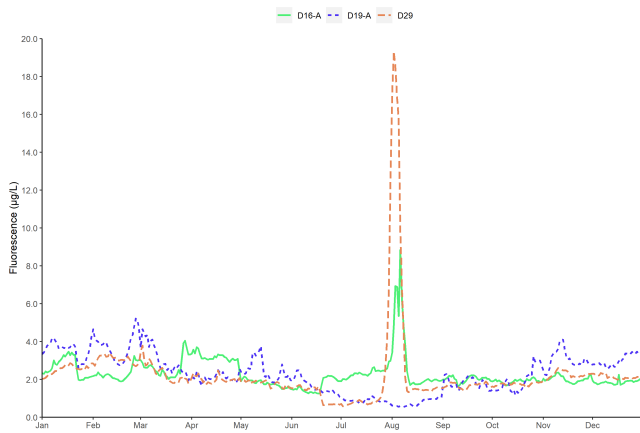


Figure 2.31: Average daily fluorescence in the Central Delta, 2020

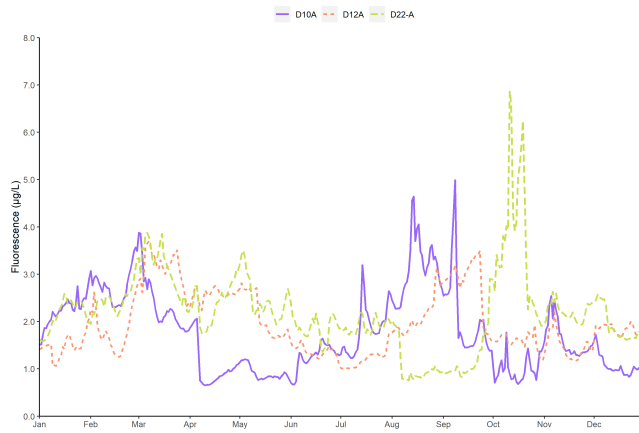


Figure 2.32: Average daily fluorescence in the Confluence, 2020

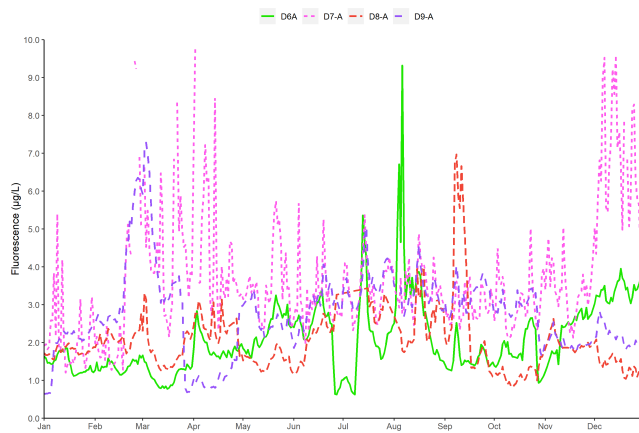


Figure 2.33: Average daily fluorescence in the Grizzly/Suisun Bays, 2020

2.2.5 References

[CVRWQCB] Central Valley Regional Water Quality Control Board. (1998). Water Quality Control Plan for the California Regional Water Quality Control Board Central Valley Region, the Sacramento River Basin, and San Joaquin River Basin [Basin Plan] (4th ed.).

[SWRCB] State Water Resources Control Board. (1995). Water Quality Control Plan for the San Francisco Bay/Sacramento-San Joaquin Estuary [Bay-Delta Plan] (Adopted May 22, 1995, pursuant to Water Right Order 95-1). Sacramento, CA.

[SWRCB] State Water Resources Control Board. (1999). Water Rights Decision 1641 for the Sacramento-San Joaquin Delta and Suisun Marsh (Adopted December 29, 1999, Revised in Accordance with order WR2000-02 March 15, 2000). Sacramento, CA.

2.3 Contact Info

For questions related to EMP's continuous water quality data sets, please contact Scott Waller at scott.waller@water.ca.gov.

Chapter 3

Discrete Water Quality

Background

Water quality is a measure of chemical and physical water conditions relative to the needs for aquatic and human life and is closely linked to the surrounding ecosystem and land use. Aquatic plants require suitable light, nutrients, and water temperatures to survive. Aquatic organisms need dissolved oxygen to breathe, and rely on adequate water temperature, salinity, and pH to survive. Humans need fresh water for recreation, irrigation, as well as to drink. Because of these competing needs, water quality is not easily defined as “good” or “bad,” since it depends on who is using it. However, water quality monitoring is a way for scientists to understand the health of our aquatic ecosystem and to help balance the needs of all who use it.

Typically, water quality is defined by regulated standards set by a regulatory agency, like the State Water Resources Control Board (SWRCB). If water quality does not meet the regulated standards, then it can be defined as poor. Water quality can be monitored continuously or in a discrete manner, both of which are done by the Environmental Monitoring Program. Discrete water quality monitoring is conducted less frequently than continuous and provides a snapshot into the water conditions at a single moment in time, which is helpful for documenting long-term trends. This type of sampling involves collecting a large quantity of water samples on a monthly basis to be analyzed for numerous water quality tests by a chemical laboratory. The Environmental Monitoring Program monitors 24 fixed discrete water quality stations within the San Francisco Estuary. These stations are sampled monthly at high water slack tide and are primarily accessed by the Research Vessel Sentinel, or by vehicle transport for shore-based stations. Sampling at each of these stations consists of collecting a variety of physical parameters (e.g. water temperature and pH) and grab samples for laboratory analysis (e.g. nitrogen and phosphorous).

Analytes

EMP collects data for six different field parameters and 18 different laboratory constituents. The analytes highlighted in this report are:

- Specific Conductance
- Turbidity
- Dissolved Ammonia
- Chlorophyll a
- Dissolved Nitrate+Nitrite
- Total Phosphorus

Sites

To analyze discrete water quality trends, the 24 fixed EMP stations are grouped into six regions of the San Francisco Bay-Delta estuary: San Pablo Bay, Suisun and Grizzly Bay, Confluence, Central Delta, Southern Interior Delta, and Northern Interior Delta. Their locations are displayed below.

3.1 Current Report

3.1.1 Introduction

Water year 2020 was classified as Dry in the Sacramento Valley and San Joaquin Valley, unlike the previous year, which was classified as Wet (source). The 2019-2020 data from all stations within the same region were plotted on one graph and then combined with the graphs from other regions to make a facet graph for each parameter. The minimum and maximum values in 2020 were determined for each field parameter or laboratory analyte to show the range within a single year. The instances when a result fell below the reporting limit were excluded from these minimum and maximum calculations. When this occurred, a vertical dashed line capped at the reporting limit was added to the graph to represent the presence of a non-detect. It should be noted that sampling was not conducted in April, May, and some of December 2020 due to the stay-at-home order and safety concerns caused by the COVID-19 pandemic. *** ### Specific Conductance

Surface specific conductance varied greatly in 2020 across the sampling regions with the highest levels occurring in the western regions (San Pablo Bay, Suisun & Grizzly Bays, Confluence) due to the strong marine influence from the Pacific Ocean. Surface specific conductance ranged from an average of 134 $\mu\text{S}/\text{cm}$ (C3A in Northern Interior Delta, July) to 45,349 $\mu\text{S}/\text{cm}$ (D41 in San Pablo Bay, November) during 2020. Higher specific conductance values were seen in 2020 ($u = 11,310 \mu\text{S}/\text{cm}$) than in 2019 ($u = 6,702 \mu\text{S}/\text{cm}$), which was likely due

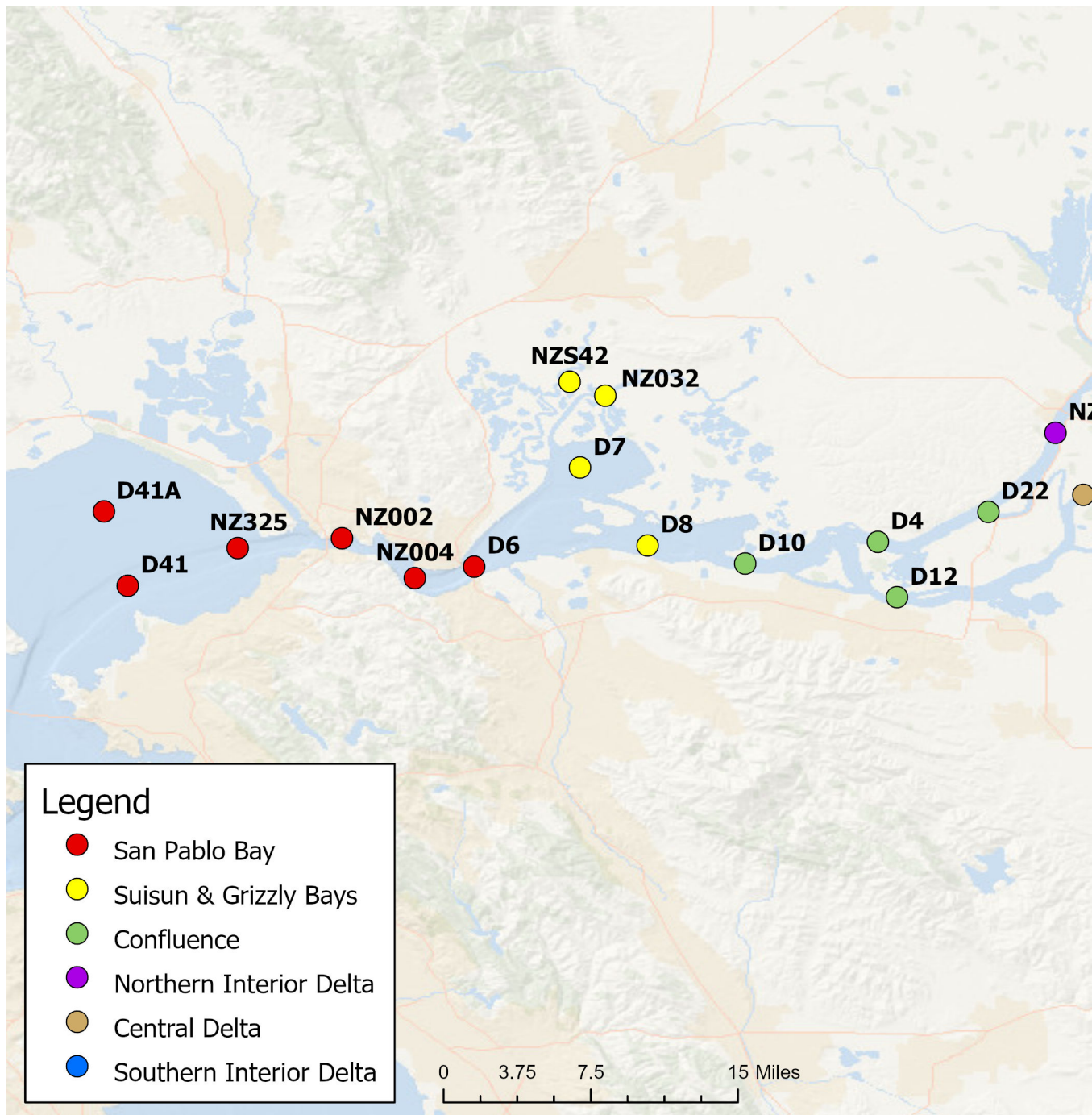


Figure 3.1: Map of EMP's field sites.

to the on-going drought keeping the San Francisco Estuary drier throughout the year.

3.1.2 Turbidity

Surface turbidity values ranged from 0.3 FNU (D19 in Central Delta, March) to 41.4 FNU (D7 in Suisun & Grizzly Bays, November) during 2020. The year 2020 had lower average turbidity than in 2019 (9.8 FNU vs. 19.6 FNU), likely due to the drought conditions that result in lack of rainfall and snowpack runoff during the winter months.

3.1.3 Dissolved Ammonia

Dissolved ammonia levels in 2020 ranged from 0.05 mg/L (the reporting limit) in several regions to 0.7 mg/L (C3A in Northern Interior Delta, March and June). Dissolved ammonia levels are typically higher at C3A in the Northern Interior Delta due to its location downstream of the effluent discharge from Sacramento Regional Sanitation District. Ammonia levels are typically lower throughout the Delta and Bays, likely due to dilution and nitrification.

3.1.4 Chlorophyll a

Chlorophyll a values in 2020 ranged from 0.53 µg/L (C3A in the Northern Interior Bay, November and NZ325 in San Pablo Bay, March) to 32.5 µg/L (C10A in Southern Interior Delta, July). The highest levels of chlorophyll a were seen in the Southern Interior Delta region during the summer months in 2020. This was mostly due to elevated levels at station C10A, which is known for being shallow during dry periods of the year, with increased temperatures and lower flows allowing for increased phytoplankton production. These elevated chlorophyll a levels in the summer at C10A also align with the continuous fluorescence data collected at this station. More information about the phytoplankton genera is described in the phytoplankton section. Average chlorophyll levels across all regions were similar in 2020 to those in 2019 (2.84 µg/L vs. 2.28 µg/L).

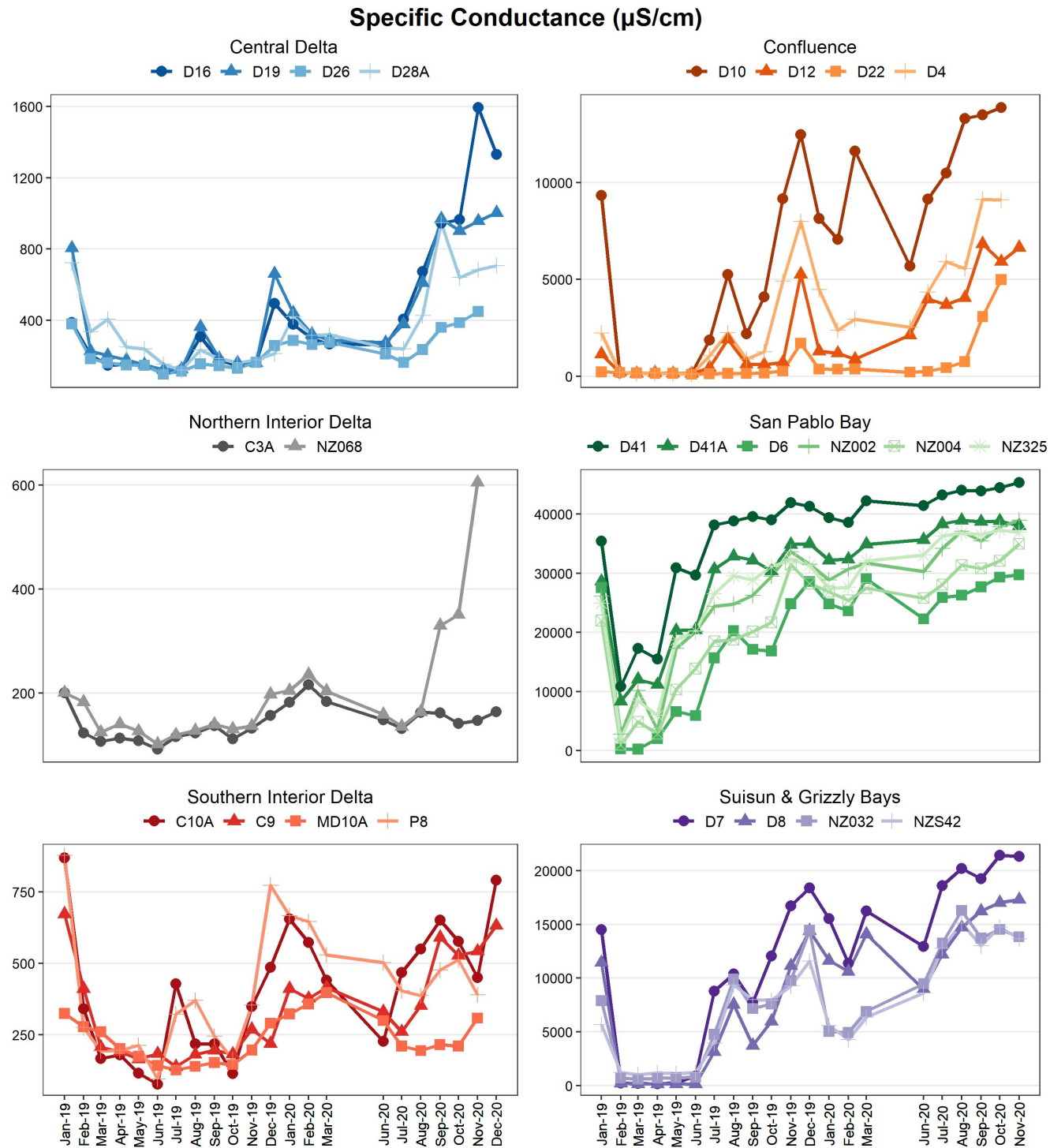


Figure 3.2: Surface specific conductance in $\mu\text{S}/\text{cm}$ at six regions in the San Francisco Bay-Delta estuary during 2019-2020.

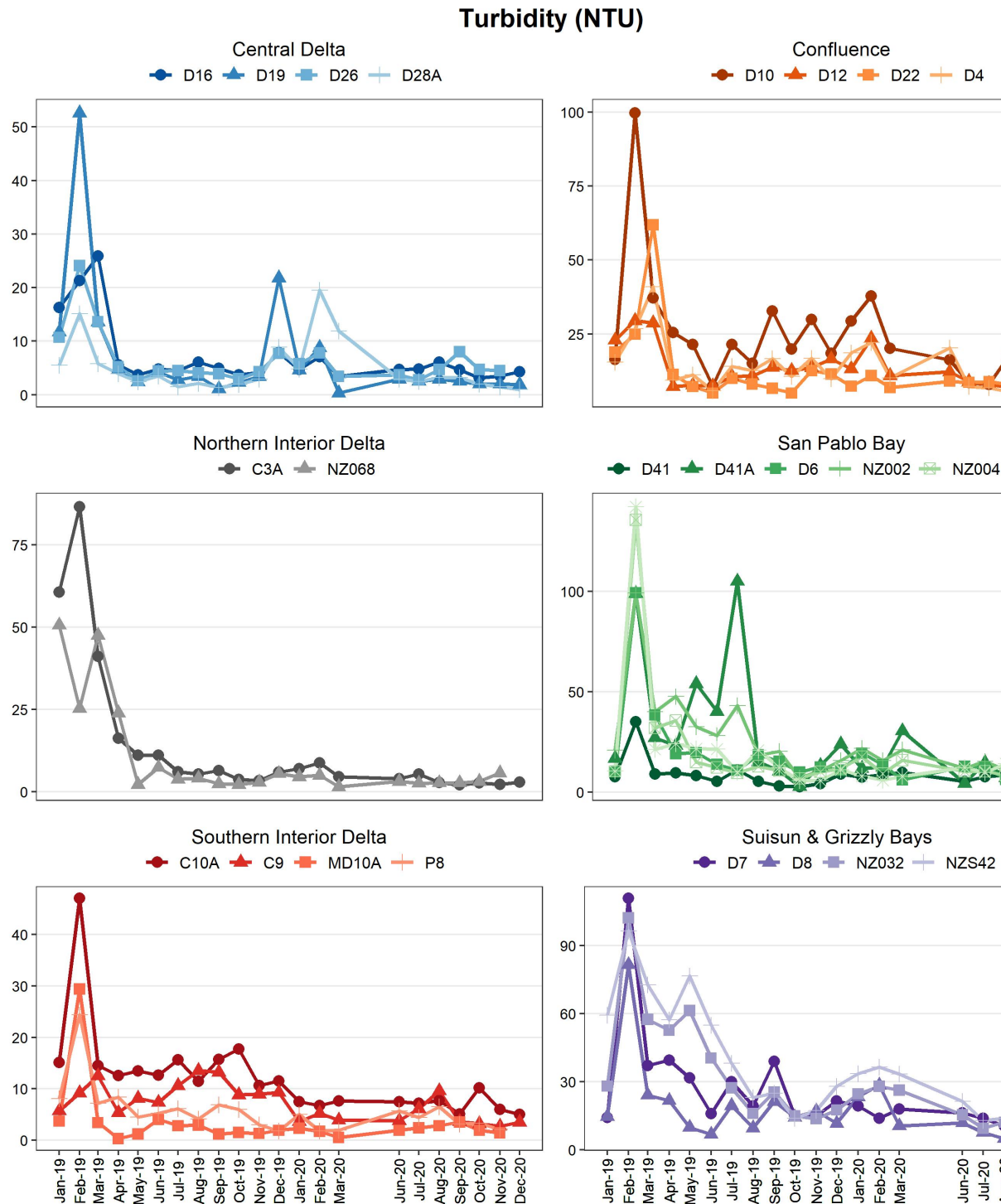


Figure 3.3: Surface turbidity in NTU at six regions in the San Francisco Bay-Delta estuary during 2019-2020.

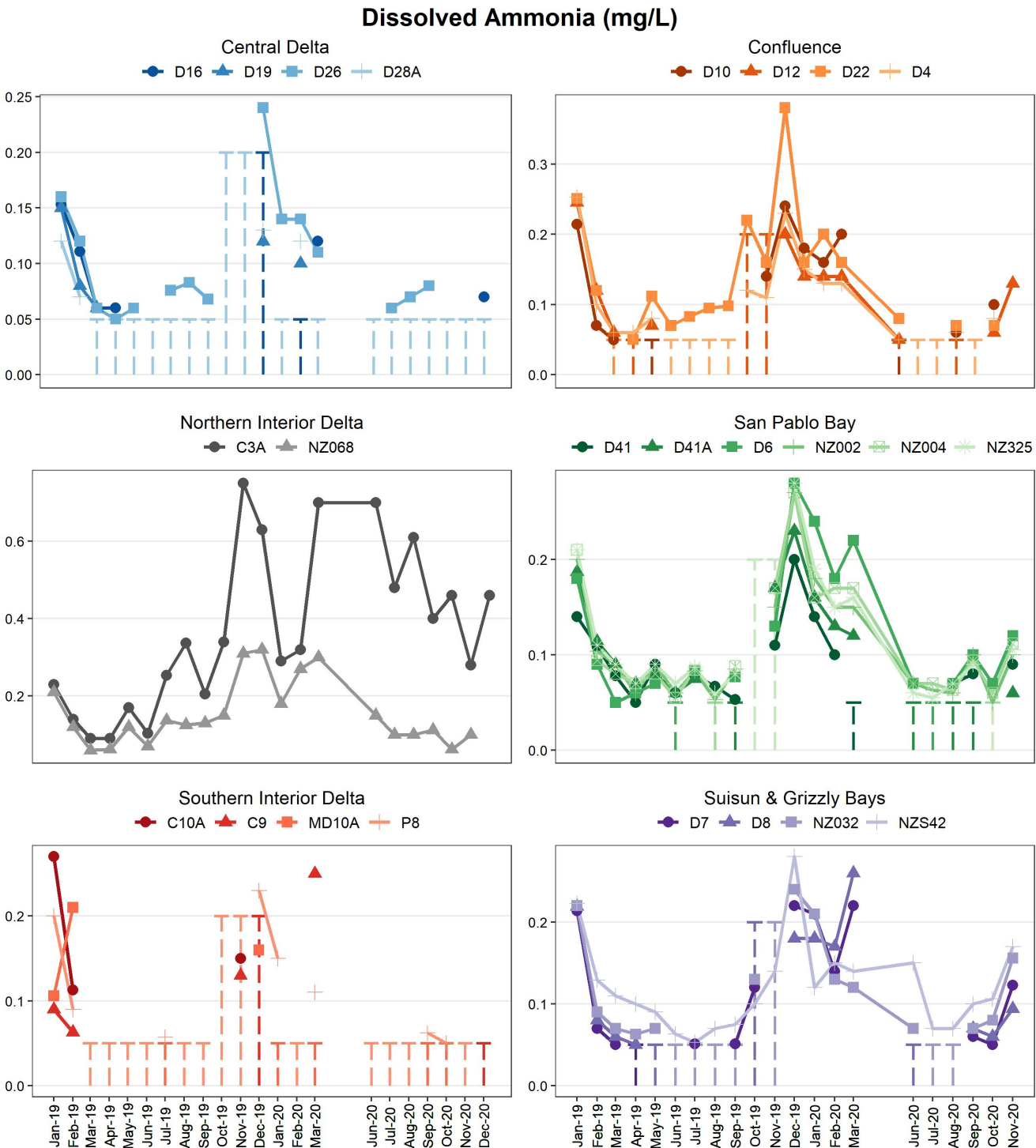


Figure 3.4: Dissolved ammonia concentrations in mg/L at six regions in the San Francisco Bay-Delta estuary during 2019-2020. Dashed lines represent the range of possible values for months where the raw value was a non-detect.

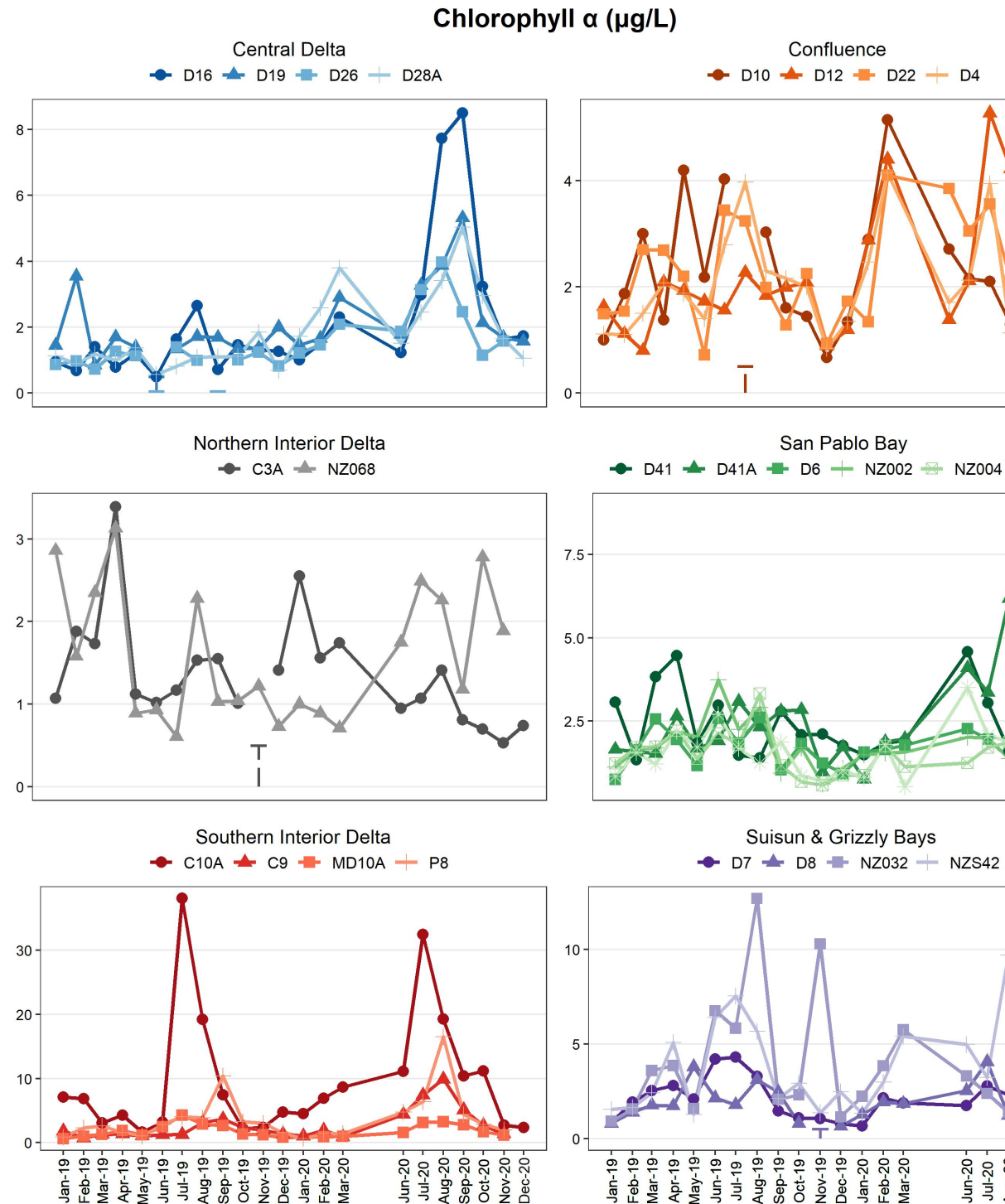


Figure 3.5: Chlorophyll α concentrations in $\mu\text{g/L}$ at six regions in the San Francisco Bay-Delta estuary during 2019-2020. Dashed lines represent the range of possible values for months where the raw value was a non-detect.

3.1.5 Dissolved Nitrate + Nitrite

Dissolved nitrate + nitrite values ranged from 0.05 mg/L (the lowest reporting limit) to 3.5 mg/L (P8 in Southern Interior Delta, October) in 2020. The Southern Interior Delta region had the highest fluctuation of dissolved nitrate + nitrite concentrations and had the highest levels compared to the rest of the estuary, likely due to influence from nearby agricultural land use and wastewater treatment effluent. Reporting limits for dissolved nitrate + nitrite were as high as 7.5 and 15 mg/L for western regions in late 2019 due to chloride influence on the analytical method. These reporting limits were cropped out of graphs for scale.

3.1.6 Total Phosphorus

In 2020, total phosphorous levels ranged from 0.04 mg/L (D28A in Central Delta, December) to 0.49 mg/L (P8 in Southern Interior Delta, September). Total phosphorus concentrations were overall similar compared to 2019 (both averaging 0.10 mg/L).

3.2 Data and Archived Reports

EMP's discrete water quality data sets are available publically via the Environmental Data Initiative (EDI) [here](#).

Archived annual reports can be found [here](#) (link currently broken).

For questions related to EMP's discrete water quality data sets, please contact Morgan Martinez at Morgan.Martinez@water.ca.gov.

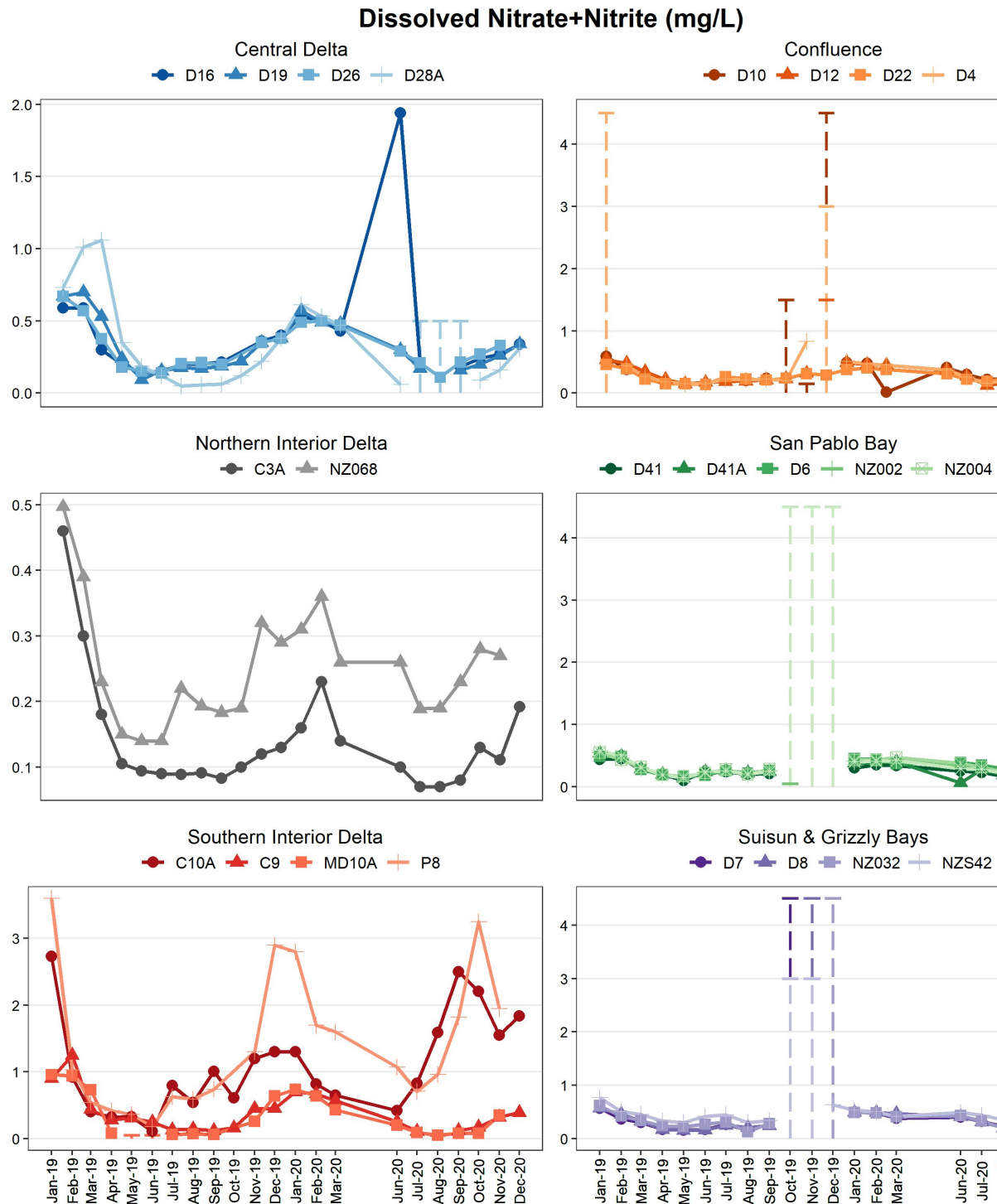


Figure 3.6: Dissolved nitrate and nitrite concentrations in mg/L at six regions in the San Francisco Bay-Delta estuary during 2019-2020. Dashed lines represent the range of possible values for months where the raw value was a non-detect.

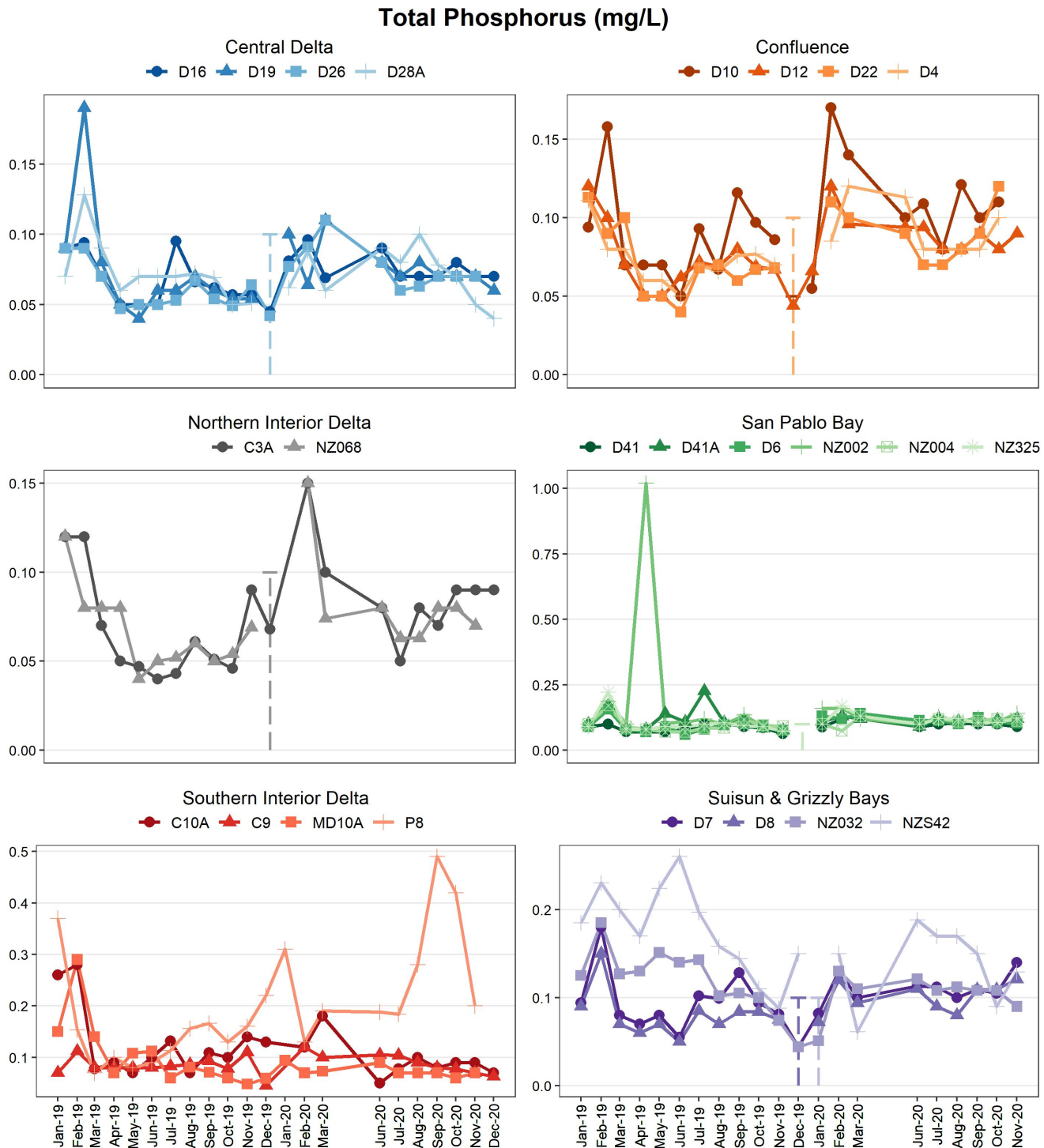


Figure 3.7: Total phosphorous concentrations in mg/L at six regions in the San Francisco Bay-Delta estuary during 2019-2020. Dashed lines represent the range of possible values for months where the raw value was a non-detect.

Chapter 4

Benthic Invertebrates

Background

Benthic organisms are creatures that live at the bottom of water bodies. This includes invertebrates (animals without backbones) like clams, shrimp, crabs, worms, aquatic insects, and small crustaceans called amphipods. Some benthic organisms live in or on the soft mud of the San Francisco Estuary, while others attach themselves to rocks and other hard surfaces. There are also benthic vertebrates (animals with backbones) that include various fish species.

Benthic organisms are a central part of the estuarine food web, consuming and consumed by other creatures. Every winter during low-tides, thousands of migrating shorebirds feast upon uncovered clams, crabs, and worms found in the mudflats. Humans can also take advantage of the low tides to harvest these organisms. Certain fish species, including juvenile salmon, striped bass, and sturgeon, also consume many types of benthic organisms.

A large percentage of the benthic organisms found in the San Francisco Estuary are non-native, and some of these species can have negative effects on the health of the estuary. For example, non-native clams can filter out much of the available phytoplankton, outcompeting the zooplankton who in turn are major sources of fish food. Historically, shrimp supported a large commercial fishery in San Francisco Estuary, and California's commercial Dungeness crab fishery still depends upon crabs that spend the first two years of their life growing in the San Francisco Estuary.

Changes in benthic organisms' populations can be indications of larger changes in the physical conditions and water quality of the San Francisco Estuary, including alterations in pollution levels, freshwater inflows, salinity, and sediment composition.

Monitoring

The Environmental Monitoring Program (EMP) has been sampling benthic invertebrates in the San Francisco Estuary since 1975. The benthic monitoring program is one element of DWR's and USBR's Environmental Monitoring Program (EMP) conducted under the Interagency Ecological Program (IEP) umbrella. The EMP also includes monitoring of water quality, zooplankton and phytoplankton. The overall objective of the benthic monitoring program is to determine the impacts of water project operations on the estuary. These impacts are interpreted by changes in benthic fauna presence, abundance and distribution associated physical factors in the estuary. Data collected from the benthic monitoring program is also used to detect newly introduced species in the estuary.

Geographic coverage of the sampling sites ranges from San Pablo Bay east through the upper Estuary to the mouths of the Sacramento, Mokelumne and San Joaquin rivers (see Figure 42). The study area currently comprises ten sites that are sampled monthly. These sites represent a wide variety of habitats that vary in size and physical make-up as well as water quality and sediment composition. The aquatic habitats sampled range from narrow, freshwater channels in the Delta to broad, estuarine bays. The mixing of river water with tidal water creates a wide range of water quality conditions. For example, salinity ranges from freshwater to around 29 ppt in the most western sites.

A 0.052 m² Ponar dredge is used to sample the benthic sediment, and all organisms larger than 0.5 mm are identified and enumerated by taxonomy contractors. To date, 414 species in ten phyla (Cnidaria, Platyhelminthes, Nemertea, Nematoda, Annelida, Arthropoda, Mollusca, Chordata, Phoronida and Echinodermata) have been collected from the study area. Sediment composition data are also collected as part of the benthic monitoring program to document general trends in sediment composition for all sites where benthic samples are collected.

4.1 Metadata

Period of Record

Benthic monitoring began in 1975. From 1975 through 1979 the program collected samples biannually from 18 to 35 stations, for a total of 48 stations over the period. In reviewing data collected between 1975 and 1979, it became evident that semi annual monitoring was insufficient to reveal long term ecological changes as mandated by Water Right Decision 1485. In 1980, DWR revised the benthic monitoring program and began monthly sampling at nine stations. In 1995, major program revisions were implemented to the program. A review of the data collected from 1980 to 1990 recommended that across-channel sampling be reduced to a single station per location in the Delta so that the geographic

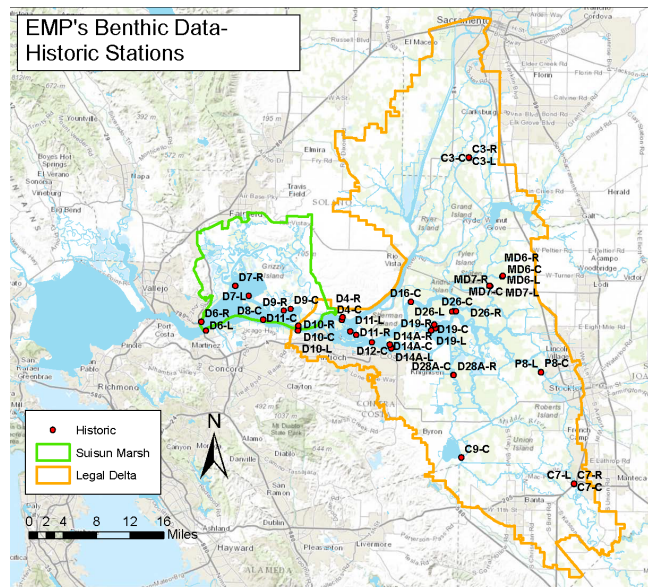


Figure 4.1: Map of EMP's benthic field sites (past and current).

coverage could be widened. These revisions included increasing the number of sites sampled each month from nine to ten and increasing the number of grab sample replicates from three to four. Detailed information about location, number and characteristics of the historical sites can be found in IEP Technical Report 12 (Markmann, 1986) and IEP Technical Report 38 (Hymanson, et al., 1994). A programmatic review of the EMP in 2001-2002 found that the benthos monitoring element was particularly in need of fundamental and comprehensive consideration through intense special studies and study design examination. Reviewers recommended a temporary reduction in sampling frequency to free up EMP resources to conduct the more spatially intense sampling without requiring additional resources. October 2003 was the last of the monthly sampling events and sampling continued quarterly (in October, January, April, July) at the stations sampled through October 2005 when monthly sampling resumed.

Sampling Frequency

Biannual sampling was conducted in late spring and fall, from 1975 to 1979. Monthly sampling started in June 1980 and ended in October 2003. Samples were collected quarterly from October 2003 through October 2005. Currently samples are collected monthly.

Sample Sites

A list of the stations at which benthic invertebrate sampling has occurred is available Note: Coordinates are in decimal degrees, and channel position is determined while facing downstream.

Field Collection Methods

Benthos { .unlisted .unnumbered }

All samples are collected using a hydraulic winch and Ponar dredge. The Ponar dredge samples a bottom area of about 0.052 m² to a depth that varies with the type of sediment and the ability of the dredge to penetrate it. Under the current program four replicate sample grabs are collected at each sampling site. The contents of the dredge are brought to the surface and placed in a large plastic bucket. Water is then added to the sample to create slurry. The contents of each grab sample bucket are washed over Standard No. 30 stainless steel mesh screen (0.595 mm openings). Each sample is carefully washed with a fine spray to remove as much of the substrate as possible. All material remaining on the screen after washing is preserved in a solution of approximately 20% buffered formaldehyde containing Rose Bengal dye for laboratory analysis. The benthic macroinvertebrate sampling methodology used in this program is described in Standard Methods for the Examination of Water and Wastewater, 20th ed. 1998 American Public Health Association, Washington D.C. (See pages 10-60 through 10-74.) | ##### Sediment { .unlisted .unnumbered } Sediment samples are also collected as part of the benthic monitoring program. Samples are collected using the same hydraulic winch and Ponar dredge as the infaunal sampling. A single sediment grab is taken at each sampling site. The contents of the Ponar dredge are emptied into a plastic tub and a random subsample is placed into a 1-liter plastic jar for storage and transport to the DWR Soils Laboratory for analysis.

Lab Processing Methods

Benthos

At the laboratory, the volume of settleable substrate in each sample jar is estimated and recorded. The formalin fixative is poured off and the sample is thoroughly washed on a 30-mesh (0.6 mm) screen. The composition of the substrate is estimated and recorded noting the relative percentages of peat, sand, mica, organic detritus, and other materials. The substrate is hand picked for organisms under a three diopter illuminated magnifier. Organisms are placed in 70% ethyl alcohol for subsequent identification. A stereoscopic dissecting microscope (70-120x) is used to identify most organisms. When taxonomic features are too small for identification under the dissecting scope, the organism is permanently mounted on a slide and examined under a compound microscope. If more than

four hours of picking is required, and a sample contains many organisms but few species, a one-fourth subsample is chosen at random. The subsample is picked and the results are multiplied by four to represent the total sample. The remainder of the sample is inspected to make sure no other taxa were overlooked. Laboratory identification and enumeration of macro-benthic organisms in each sample is performed under contract by Hydrozoology Laboratory, P.O. Box 682 Newcastle, CA 95658. Analysis has been done by Hydrozoology for the program's entire period of record.

Sediment

All sediment samples are analyzed by the DWR Soils Laboratory, West Sacramento, CA. Analysis of a sediment sample involves determining the percent size fractions with the use of a mechanical sieve. The sieves sizes are as follow: 75, 37.5, 19, 9.5, 4.75, 2.36, 1.18, 0.6, 0.3, 0.15, 0.075, 0.005, 0.002, 0.001 mm. All particle sizes are found on a regular basis in the samples with the exception of gravel (particles greater than 4.76 mm in diameter). The percent organic content of each sediment sample is also determined from the loss in weight of an oven-dried sample burned at 440 degrees Celsius for 8 hours. All laboratory analysis procedures follow the American Society for Testing Methods, D-2974, "Moisture, Ash, and Organic Matter" and D-422-63, "Particle-Size Analysis of Soil".

Works Cited

Hymanson, Z., D. Mayer and J. Steinbeck. 1994. Long-Term Trends in Benthos Abundance and Persistence in the Upper Sacramento-San Joaquin Estuary, Summary Report: 1980-1990. IEP Technical Report 38. 68 pp.

Markmann, C. 1986. Benthic Monitoring in the Sacramento-San Joaquin Delta. Results from 1975 through 1981. IEP Technical Report 12. 51 pp.

4.2 Current Report

4.2.1 Introduction

Benthic monitoring conducted by the California Department of Water Resources (DWR) since 1975 has documented changes in the composition, density, and distribution of the macrobenthic biota inhabiting the upper San Francisco Estuary. This monitoring is performed by the Environmental Monitoring Program (EMP) as part of the Interagency Ecological Program (IEP) and is one component of the biological monitoring mandated by Water Right Decision D-1641. Since benthic species respond to changes in physical factors such as freshwater inflows, salinity, and substrate composition, benthic community data provides

an indication of physical changes occurring within the Estuary. Benthic monitoring is an important component of the EMP because operation of the State Water Project can change the Estuary's flow characteristics, affecting the density and distribution of benthic biota. Benthic monitoring data is also used to detect and document the presence of new, non-native species in the Upper Estuary, such as the 1986 arrival and subsequent wide spread of the overbite clam, *Potamocorbula amurensis*. This article summarizes benthic community characteristics at EMP monitoring sites in 2020 and contextualizes these observations using community data from the preceding decade.

4.2.2 Methods

Benthic monitoring was conducted monthly at 10 sampling sites distributed throughout the Estuary, from San Pablo Bay upstream through the Sacramento-San Joaquin Delta. Sampling in April, May, and December 2020 was not conducted due to the COVID-19 pandemic. EMP staff collected five bottom grab samples at each station using a Ponar dredge with a sampling area of 0.052 m². Four replicate grab samples were analyzed for benthic macrofauna and the fifth sample was analyzed for sediment composition. Benthic macrofauna samples were analyzed by Hydrozoology, a private laboratory under contract with DWR. All organisms were identified to the lowest taxon possible and enumerated. Sediment composition analysis was conducted at the DWR Soils and Concrete Laboratory. Field collection methodology and laboratory analysis of benthic macroinvertebrates and sediment composition are described in detail in the benthic metadata found at <https://emp-des.github.io/emp-reports/benthic-meta.html>

Prior to analysis, the units for individual organisms were transformed from count data to densities of individuals per square meter, and the average density was calculated across the four replicate grabs at each site. Species were then grouped by phyla, and time series for each station were constructed to depict seasonal patterns in benthic communities. Rare phyla (< 5% of the total organisms for the given year) were omitted from the plots. We did not report sediment compositions for 2020 because the data for most months was not yet available, due to delays from the COVID-19 pandemic.

The 2020 water year was designated as “Dry” for both the Sacramento Valley and the San Joaquin Valley according to the DWR’s Water Year Hydrologic Classification Indices. Benthic communities in 2020 were expected to be like previous “Dry” and “Critically Dry” years (most recently during the 2013-2016 drought) and differ from years designated Wet or Above Normal both in species composition and in species abundances.

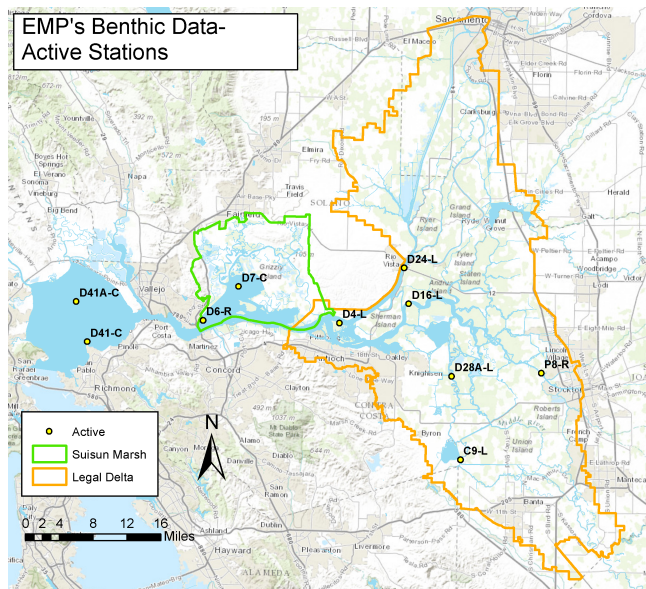


Figure 4.2: Map of EMP's current benthic field sites.

4.2.3 Results

The benthic fauna collected in 2020 comprised nine phyla: Mollusca (40% of total organisms), Arthropoda (40%), and Annelida (19%), with Phoronida, Nemotoda, Nemertea, Platyhelminthes, Chordata, and Cnidaria each representing < 1% of total organisms. Of the 180 benthic species collected in 2020, the ten most abundant species represented 83% of all individuals collected throughout the year (Table 1). These include four species of amphipod, two clams, two oligochaete worms, and two polychaete worms. Only one species in this group (the amphipod *Americorophium spinicorne*) is known to be native to this estuary; all others are non-native or are cosmopolitan species of unknown origin. Refer to Fields and Messer (1999) for descriptions of the habitat requirements, physical attributes, and feeding methods of many of these species.

In the site descriptions that follow, most species densities are reported as the annual densities of individuals/m², sometimes noting dramatic seasonal peaks. Some species, especially arthropods, display strong seasonal variability, with peak monthly densities several times higher than their annual densities. In these cases, we reported the time and magnitude of the peaks as well as the annual densities. Please note, however, that the reported annual densities omit three months of 2020 (April, May, and December) when sampling did not occur, and

Species	Organism Type	Native/ introduced status	Station(s) at which species was found*	Month(s) in which species was abundant**	Total number of individuals***
<i>Potamocorbula amurensis</i>	Clam	Introduced	D6, D7	All months	53,436
<i>Ampelisca abdita</i>	Amphipod	Introduced	D41, D41A	June-October	35,344
<i>Corbicula fluminea</i>	Clam	Introduced	D24, D28A, D4, P8, C9, D16	All months	13,758
<i>Americorophium spinicorne</i>	Amphipod	Native	D4, P8	February-July	12,257
<i>Varichaetodrilus angustipennis</i>	Oligochaete worm	Introduced	C9, D4, D28A, P8	All months	11,152
<i>Sinocorophium alienense</i>	Amphipod	Introduced	D7	January-September January-March, September-November	8,931
<i>Manayunkia speciosa</i>	Polychaete worm	Introduced	D28A, P8	January-March, September-November	5,626
<i>Gammarus dubius</i>	Amphipod	Introduced	D24, D4, D28A, P8	June-July, November	5,465
<i>Limnodrilus hoffmeisteri</i>	Oligochaete worm	Unknown; cosmopolitan	C9, P8, D4, D28A	All months	4,078
<i>Laonome calida</i>	Polychaete worm	Introduced	D4, C9, P8, D7, D28A	February-March, September-November	2,026

* Stations are listed in order from highest to lowest total annual abundance.

** Across all stations, abundant is defined as > 5% of total species count for the year.

*** Total number of individuals was the sum of individuals at all sites at all months in 2019.

Figure 4.3: List of ten most numerous benthic invertebrate species found at EMP sites in 2020.

comparisons to other years' annual densities or seasonal patterns should take these omissions into account. Readers who wish to see the full dataset can access it at <https://emp.baydeltalive.com/>.

4.2.4 San Pablo Bay

The most saline of our sites, D41 and D41A, are polyhaline sites in San Pablo Bay. At D41 in 2019, the most numerous species was the non-native clam *Potamocorbula amurensis*, whose density peaked in July to 12,587 individuals per square meter, in a pattern seen primarily in wet years. Site D41 was also notable as the only site where we saw phoronids, also known as horseshoe worms, which are only found in this higher-salinity site.

At D41A, there were high densities of the non-native amphipod *Ampelisca abdita*, which had a high of 9,846 individuals/m² in December 2019, as well as *Potamocorbula amurensis* with an average annual density of 1,686 individuals/m².

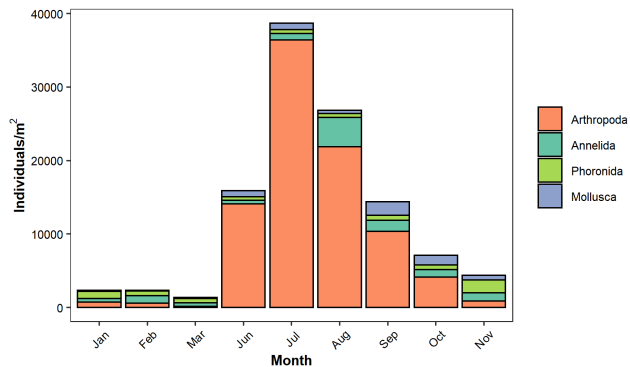


Figure 4.4: Density of benthic organisms, by month, collected at station D41 in 2019.

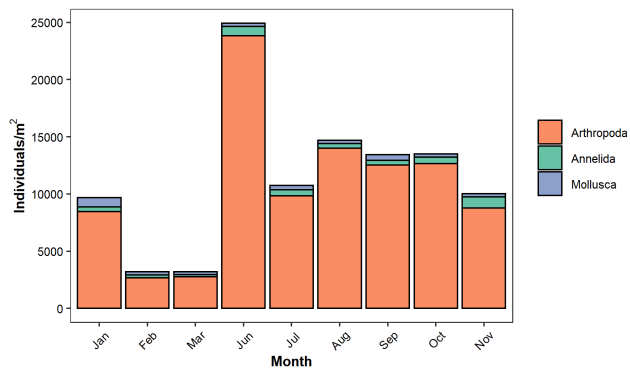


Figure 4.5: Density of benthic organisms, by month, collected at station D41A in 2019.

4.2.5 Suisun and Grizzly Bay

In Suisun Bay and Grizzly Bay in 2019, our mesohaline sites D6 and D7 both saw high numbers of the invasive clam *P. amurensis*, which had an average density of 9,891 individuals/m² and comprised 97% of all organisms at D6 in 2019, similar to other recent years. At D7, *P. amurensis* had a September peak of 12,471 individuals/m², and the non-native amphipod *Corophium alienense* had a November peak of 10,428 individuals/m². These two species together made up 94% of all organisms at D7 in 2019.

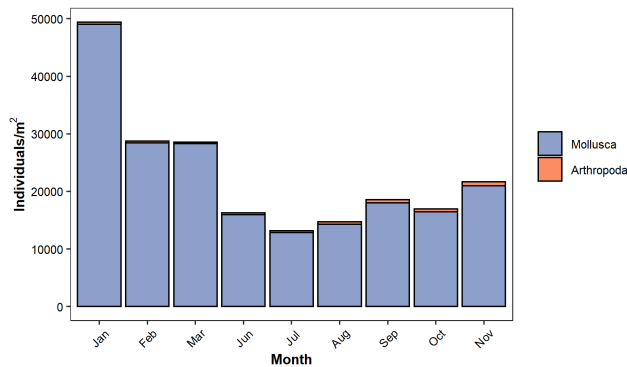


Figure 4.6: Density of benthic organisms, by month, collected at station D6 in 2019.

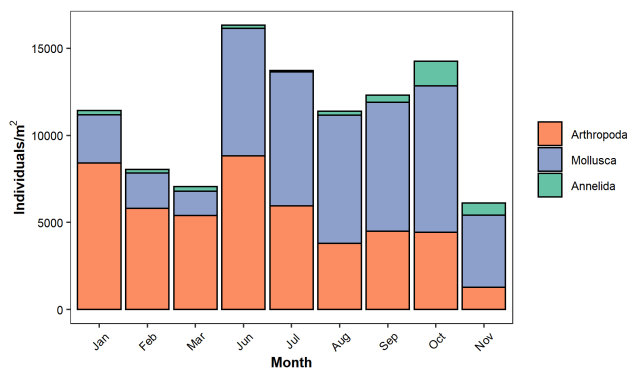


Figure 4.7: Density of benthic organisms, by month, collected at station D7 in 2019.

4.2.6 Confluence

At the confluence of the Sacramento and San Joaquin rivers, site D4's oligohaline community was comprised in 2019 largely of the amphipods *Americorophium spinicorne* and *Gammarus daiberi*, which each had high variability through the year. The oligochaete worm *Varichaetadrilus angustipenis* also had high density in the second half of the year.

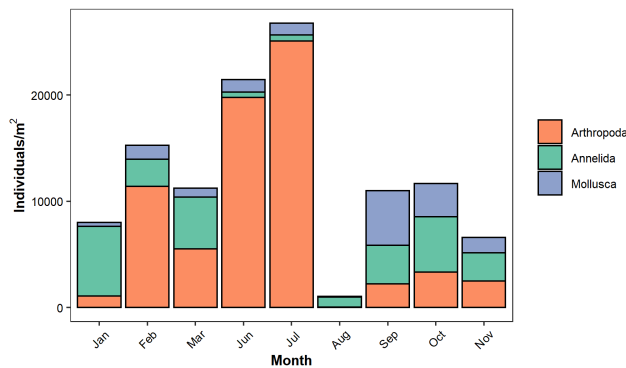


Figure 4.8: Density of benthic organisms, by month, collected at station D4 in 2019.

4.2.7 Central Delta

In the Sacramento River, freshwater site D24 was dominated by the non-native clam *Corbicula fluminea*, whose numbers averaged 3,016 per square meter over the course of 2019, similar to the very high densities of 2018. There was also a significant seasonal increase in densities of the amphipod *Gammarus daiberi* between September and December.

In the San Joaquin River, freshwater site D16 (at Twitchell Island) was dominated in 2019 by the amphipod *Gammarus daiberi*, which demonstrated an impressive density peak in May, as well as the clam *Corbicula fluminea* and the oligochaete worm *V. angustipenis*.

In Old River, freshwater site D28A had a diverse community in 2019. There were high densities of the ostracod crustacean *Cyprideis* sp. A and the sabellid worm *Manayunkia speciosa* at the beginning of the year and lower densities for most of the rest of 2019. There were also seasonal peaks of the oligochaete worm *V. angustipenis* and the amphipods *G. daiberi* and *A. spinicorne*.

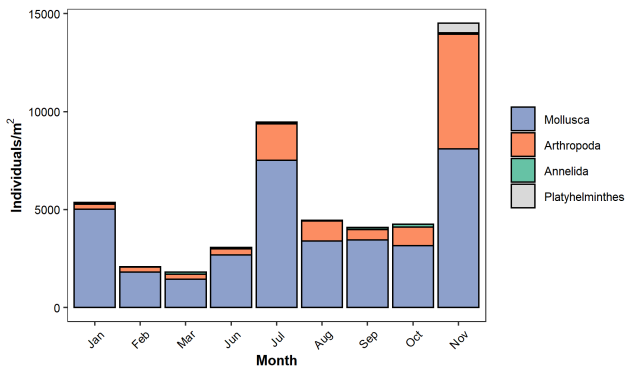


Figure 4.9: Density of benthic organisms, by month, collected at station D24 in 2019.

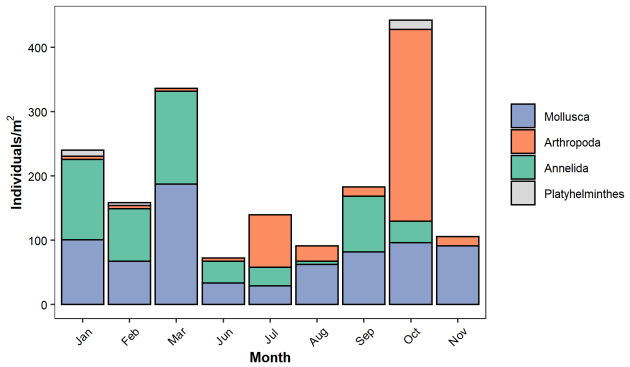


Figure 4.10: Density of benthic organisms, by month, collected at station D16 in 2019.

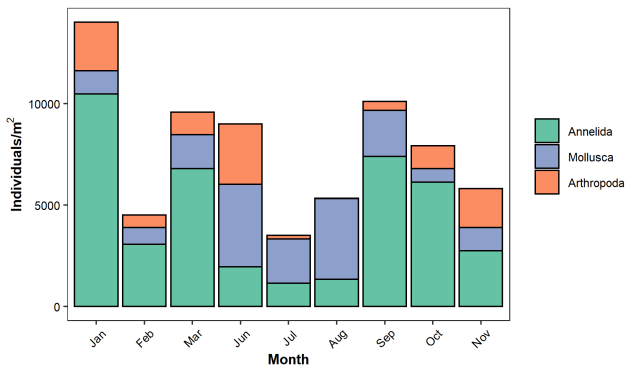


Figure 4.11: Density of benthic organisms, by month, collected at station D28A in 2019.

4.2.8 Southern Interior Delta

Further upstream in the San Joaquin River, site P8 at Buckley Cove was dominated by the sabellid worm *M. speciosa* which saw peaks in October and March. In addition to this species, which accounted for 59% of all organisms, site P8 saw a diverse community of freshwater oligochaetes, aquatic insects, and amphipods in addition to the non-native clam *C. fluminea*.

At Clifton Court Forebay, freshwater site C9 was dominated by a number of annelid species in 2019. *Varichaetadrilus angustipenis*, *Limnodrilus hoffmeisteri*, and *Ilyodrilus frantzi* were present at high densities throughout the year, at moderately higher levels than in 2018. The amphipod *Hyalalla sp. A* experienced a dramatic peak in density in November and December (Figure 52). Site C9 is regularly one of our most biodiverse sites, with an additional large number of species present at low densities.

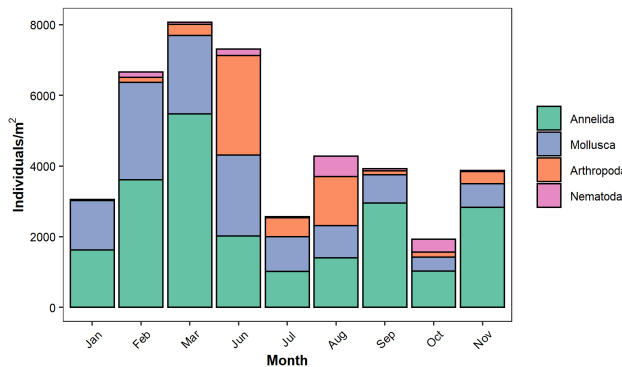


Figure 4.12: Density of benthic organisms, by month, collected at station P8 in 2019.

4.2.9 Summary

In summary, 2019 saw an overall decrease in invasive clam density from 2018 (13% for *P. amurensis* and 10% for *C. fluminea*). Other notable features of 2019 were the sharp decrease in overall density of the amphipod *A. abdita* in Grizzly Bay, after reaching a decadal peak in 2018, likely due to 2019's decreased salinity, as well as the 2019 increase in the annelid *M. speciosa*, after its steady decrease from 2015 – 2018. Our ability to recognize these changes highlights the importance of monitoring benthic invertebrates to a high taxonomic resolution across the entire estuarine salinity gradient since the community has important interactions with various abiotic conditions as well as key parts of the estuarine food web.

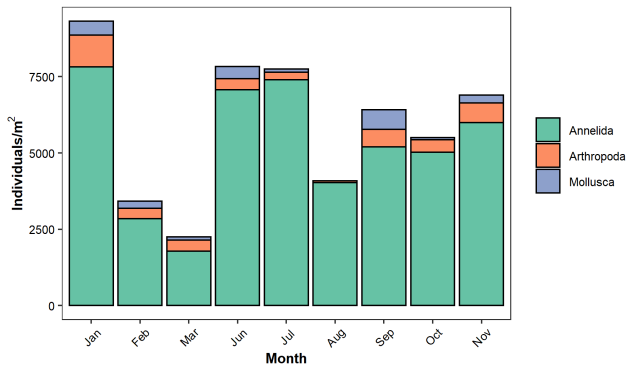


Figure 4.13: Density of benthic organisms, by month, collected at station C9 in 2019.

4.3 Data and Archived Reports

EMP's benthos data sets are available to download

Archived annual reports can be found here (link currently broken).

For questions related to EMP's benthos data sets, please contact Betsy Wells
at elizabeth.wells@water.ca.gov.

Chapter 5

Phytoplankton

Background

What are Phytoplankton?

Phytoplankton are small organisms that can be found floating in most water bodies. They occur as unicellular forms (single cell), colonial forms (multiple cells in a clump), filaments (long chains of cells), or flagellates (having flagella that give them some mobility). Like plants, they are primary producers; they convert light energy from the sun and carbon dioxide into the living matter of their cells through photosynthesis. Phytoplankton from the San Francisco Estuary fall into four broad categories: cyanobacteria, diatoms, green algae, and various flagellate groups.

- Cyanobacteria are the only phytoplankton that are true bacteria, meaning their cells' internal structures do not have membranes around them. Often called blue-green algae due to their color, they have colonized nearly all freshwater, marine, and terrestrial habitats on earth. Some species can produce blooms and harmful toxins that degrade water quality.
- Diatoms are unique among phytoplankton because they have a cell wall made of glass, or silicon dioxide, called a frustule. They can be unicellular or colonial. There are two main types of diatoms, centric and pennate.
- Green algae are a large, diverse group of phytoplankton consisting of unicellular, filamentous, colonial, and flagellated forms. They are found in a wide variety of freshwater, marine, and terrestrial habitats. Some species can form nuisance blooms or surface scums in nutrient-rich water.
- Flagellates include phytoplankton from many different groups, such as cryptophytes, dinoflagellates, chrysophytes, haptophytes, and euglenoids. Some flagellates, like cryptophytes, can be important as food for zooplankton. Some groups of flagellates, such as haptophytes and dinoflagellates, can produce toxic blooms that can kill or poison fish and invertebrates.

Why are phytoplankton important?

Phytoplankton are the foundation of the aquatic food web. They feed a diverse array of organisms, ranging from microscopic zooplankton to large pelagic fish. Small fish and benthic organisms also graze on phytoplankton, and are in turn consumed by larger organisms such as birds. Because of their importance as the base of the food web, changes in phytoplankton in the San Francisco Estuary can have cascading effects throughout the food web. For example, loss of phytoplankton species that are important food sources can negatively affect the zooplankton and fish species that feed on those phytoplankton, and thus negatively affect the animals preying on those zooplankton and fish.

Phytoplankton can also affect elements of water quality such as pH, dissolved oxygen, taste and odor of drinking water, and water transparency. Large algal blooms, both toxic and non-toxic, can have adverse effects on the water quality parameters listed above. They can also have negative aesthetic effects by forming large, floating surface scums. Monitoring changes in phytoplankton can be useful in assessing water quality trends by detecting the presence of nuisance species or the development of large blooms that could require management action.

Chlorophyll-a is the primary photosynthetic product made by phytoplankton and plants, and gives them their green color. Chlorophyll-a is also a measure of the biomass that is directly available to organisms that prey on phytoplankton, such as clams and zooplankton.

Sometimes the green color is masked by secondary pigments, and these phytoplankton often appear brown or red instead of green. Phytoplankton biomass and the resulting chlorophyll-a concentrations in some areas of the Estuary may be influenced by extensive filtration of the water column by the introduced Asian clam, *Potamocorbula amurensis*. Well-established benthic populations of *P. amurensis* in Suisun and San Pablo bays are thought to have contributed to the low chlorophyll-a concentrations (and increased water clarity) measured in these westerly bays since the mid-1980s. By removing phytoplankton from the water, *P. amurensis* has reduced the amount of phytoplankton available to other organisms such as zooplankton.

Department of Water Resources Phytoplankton and Chlorophyll-a Monitoring

How is phytoplankton monitored?

The California DWR Phytoplankton and Chlorophyll-a monitoring measures the composition (what kinds?), abundance (how many?), diversity (how many kinds?), and distribution (where are they?) of phytoplankton. It also measures phytoplankton biomass as chlorophyll-a; both types of monitoring are performed as part of the IEP's Environmental Monitoring Program (EMP). Thirteen fixed

Table 5.1: Stations included within each region of the Delta

Region	Stations
Nothern Interior Delta	C3A and NZ068
Southern Interior Delta	C9, C10A, MD10A and P8
Central Delta	D16, D19, D26 and D28A
The Confluence	D4, D10, D12 and D22
Grizzly and Suisun Bay	D7, D8, NZ032 and NZS42
San Pablo Bay	D6, D41, D41A, NZ002, NZ004 and NZ325

sites are currently sampled for both phytoplankton and chlorophyll-a (Table 5.1), with two additional sites sampled at variable locations based on bottom specific conductance of 2,000 and 6,000 micro-Siemens, respectively. Historically, samples were collected once or twice monthly at up to 33 sites. Phytoplankton and chlorophyll-a samples are collected monthly alongside the water quality and zooplankton sampling. Whole, unfiltered water samples are collected monthly from one meter below the surface to determine phytoplankton composition; Lugol's solution is then added as a stain and preservative. For chlorophyll-a samples, water is filtered onto glass carbon fiber filters for analysis. Phytoplankton and chlorophyll-a data are available from 1975 to the present.

Changes in phytoplankton composition, abundance, diversity, distribution, and biomass are monitored throughout the San Francisco Estuary, from San Pablo Bay east through the upper Estuary to the mouths of the Sacramento, Mokelumne, and San Joaquin Rivers.

Because different phytoplankton species live in different parts of the Estuary, the sites represent a wide range of habitats of varying physical conditions, including wide ranges of salinity and temperature. Sites range from narrow, freshwater channels in the Delta to broad, estuarine bays.

5.1 Current Report

5.1.1 Introduction

The Department of Water Resources (DWR) and the US Bureau of Reclamation (USBR) are required by Water Right Decision 1641 (D-1641) to collect phytoplankton and chlorophyll a samples to monitor algal community composition and biomass at select sites in the upper San Francisco Estuary (Estuary). The twenty-four sites range from San Pablo Bay to the inland rivers of the Sacramento-San Joaquin Delta ("the Delta"). These sites represent a variety

of aquatic habitats, from narrow, freshwater channels to broad, estuarine bays. This report describes the results of these monitoring efforts for calendar year 2020.

Phytoplankton are small, free-floating organisms that occur as unicellular, colonial, or filamentous forms (Horne and Goldman, 1994). Phytoplankton are a key component of the Estuary's food web, serving as food for zooplankton, invertebrates, and certain fish species. Their metabolic processes also impact water chemistry, and their ability to fix carbon through photosynthesis is one of the key processes influencing water quality in the Estuary. Via this process, phytoplankton can affect the pH, dissolved oxygen, color, taste, and odor of natural waters.

Under certain conditions, some species of phytoplankton (e.g., *Microcystis aeruginosa*) can cause harmful algal blooms (HABs), releasing toxin compounds which can be dangerous or even lethal to animals and humans (Carmichael, 1981). In freshwater, the cyanobacteria, or blue-green algae (class Cyanophyceae), are responsible for producing toxic blooms, particularly in waters that are polluted with phosphates (van den Hoek et al., 1995). Phytoplankton are also useful for assessing water quality (Gannon and Stemberger 1978); their short life cycles allow them to respond quickly to environmental changes, meaning their standing crop and species composition are indicative of source water characteristics (APHA 2012). However, because of their transient nature, patchiness, and free movement in a lotic environment, the utility of phytoplankton as water quality indicators is limited and should be interpreted in conjunction with other biological and physiochemical data (APHA 2012).

In addition to collecting phytoplankton samples to assess community composition, we use the measured concentration of chlorophyll a as a proxy to infer phytoplankton biomass. Chlorophyll molecules are complex phytopigments found in most photosynthetic organisms. There are several types of chlorophyll, which are distinguished by slight differences in their molecular structures and constituents. These include chlorophyll a, b, c, and d, with a being the principal photosynthetic pigment in most phytoplankton. This makes the chlorophyll a pigment a reliable proxy measurement for phytoplankton biomass.

In addition, we measured the concentration of a different pigment in our water samples, pheophytin a. Pheophytin a is a primary degradation product of chlorophyll a. Comparing its concentration relative to chlorophyll a is a useful metric for estimating the general physiological state of phytoplankton populations. When phytoplankton are actively growing, the concentrations of pheophytin a are normally expected to be low relative to chlorophyll a. Conversely, when the phytoplankton have died and are decaying, levels of pheophytin a are expected to be high in relation to chlorophyll a.

Phytoplankton biomass and the resulting amount of chlorophyll a in some areas of the Estuary may be influenced by extensive filtration of the water column by the introduced Asian clam, *Potamocorbula amurensis* (Alpine and Cloern 1992).

Well-established benthic populations of *P. amurensis* in Suisun and San Pablo bays are thought to have contributed to the low chlorophyll a concentrations (and increased water clarity) measured in these westerly bays since the mid-1980s (Alpine and Cloern 1992).

Phytoplankton are small, free-floating organisms that occur as unicellular, colonial, or filamentous forms (Horne and Goldman, 1994). They primarily serve as an important food source for zooplankton, invertebrates, and certain fish species, although they also have a direct effects on water chemistry. Primary production by phytoplankton, primarily via carbon fixation through photosynthesis, is one of the key processes that influence water quality in the Estuary. Via this process, phytoplankton can affect pH, dissolved oxygen, color, taste, and odor. Under certain conditions, some species (eg. *Microcystis aeruginosa*) can cause harmful algal blooms (HABs), resulting in animal deaths and human illness (Carmichael, 1981). In freshwater, the cyanobacteria, or blue-green algae (class Cyanophyceae), are responsible for producing toxic blooms, particularly in waters that are polluted with phosphates (van den Hoek et al., 1995). Phytoplankton are also useful for assessing water quality (Gannon and Stemberger 1978); their short life cycles allow them to respond quickly to environmental changes, meaning their standing crop and species composition are indicative of source water characteristics (APHA 2012). However, because of their transient nature, patchiness, and free movement in a lotic environment, the utility of phytoplankton as water quality indicators is limited and should be interpreted in conjunction with other biological and physiochemical data (APHA 2012).

In addition to collecting phytoplankton samples to assess community composition, we use chlorophyll a concentrations as proxies to calculate phytoplankton biomass. Chlorophylls are complex phytopigment molecules found in all photosynthetic organisms. There are several types of chlorophyll, which are distinguished by slight differences in their molecular structures and constituents. These include chlorophyll a, b, c, and d, with a being the principal photosynthetic pigment in the majority of phytoplankton. This makes the chlorophyll a pigment a reliable proxy measurement for phytoplankton biomass. Furthermore, water samples were analyzed for pheophytin a. Pheophytin a is a primary degradation product of chlorophyll a. Its concentration, relative to chlorophyll a, is useful for estimating the general physiological state of phytoplankton populations. When phytoplankton are actively growing, the concentrations of pheophytin a are normally expected to be low in relation to chlorophyll a. Conversely, when the phytoplankton have died and are decaying, levels of pheophytin a are expected to be high in relation to chlorophyll a.

Phytoplankton biomass and the resulting chlorophyll a concentrations in some areas of the Estuary may be influenced by extensive filtration of the water column by the introduced Asian clam, *Potamocorbula amurensis* (Alpine and Cloern 1992). Well-established benthic populations of *P. amurensis* in Suisun and San Pablo bays are thought to have contributed to the low chlorophyll a concentrations (and increased water clarity) measured in these westerly bays since the mid-1980s (Alpine and Cloern 1992).

5.1.2 Methods

5.1.2.1 Phytoplankton

Phytoplankton samples were collected monthly at 24 monitoring sites throughout the Upper Estuary, which were grouped into regions based on their geographic location. Samples were collected 1 meter below the water's surface using a submersible pump and stored in 50 mL amber glass bottles. 200 μL of Lugol's solution was added to each sample as a stain and preservative. All samples were kept at room temperature and away from direct sunlight until they were analyzed.

Phytoplankton identification and enumeration were performed by BSA Environmental, Inc. according to the Utermöhl microscopic method (Utermöhl, 1958) and modified Standard Methods (APHA, 2012). An aliquot of sample was placed into a counting chamber and allowed to settle for a minimum of 12 hours. The aliquot volume, normally 10-20 mL, was adjusted according to the algal population density and the turbidity of the sample. Phytoplankton taxa were enumerated in randomly chosen transects for each settled aliquot. This process was performed at 800x magnification using a Leica DMIL inverted microscope. For each aliquot, a minimum of 400 total algal units were counted, with the dominant taxon accounting for a minimum of 100 algal units. For filamentous or colonial taxa, the number of cells per filament or colony was recorded.

Raw organism counts were normalized to the sample volume using the following formula:

$$\text{organisms/mL} = \frac{CA_c}{VA_f F}$$

where C is the organism count, A_c is the area of the cell bottom (mm^2), A_f is the area of each grid field (mm^2), F is the number of fields examined, and V is the settled volume (mL). This simplifies to:

$$\text{organisms/mL} = \frac{C}{cV}$$

where $cV = \frac{A_c}{VA_f F}$ and is equal to the counted volume.

The 10 most common genera were determined by summing the normalized organism counts across all stations and months for each genus. For the bar graphs, average organism counts were calculated per month, per region, and normalized to the number of stations.

Raw organism counts were normalized to the sample volume using the following formula:

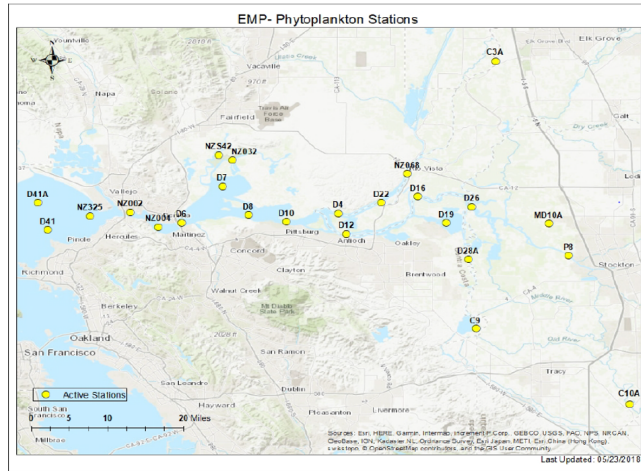


Figure 5.1: Map of phytoplankton stations sampled by the Environmental Monitoring Program

Table 5.2: Stations included within each region of the Delta

Region	Stations
Nothern Interior Delta	C3A and NZ068
Southern Interior Delta	C9, C10A, MD10A and P8
Central Delta	D16, D19, D26 and D28A
The Confluence	D4, D10, D12 and D22
Grizzly and Suisun Bay	D7, D8, NZ032 and NZS42
San Pablo Bay	D6, D41, D41A, NZ002, NZ004 and NZ325

$$\text{organisms/mL} = \frac{CA_c}{VA_f F}$$

where C is the organism count, A_c is the area of the cell bottom (mm^2), A_f is the area of each grid field (mm^2), F is the number of fields examined, and V is the settled volume (mL). This simplifies to:

$$\text{organisms/mL} = C \frac{c}{V}$$

where $cV = \frac{A_c}{VA_f F}$ and is equal to the counted volume.

5.1.2.2 Chlorophyll a and Pheophytin a

Samples of chlorophyll a and pheophytin a were collected monthly at 24 monitoring sites throughout the upper Estuary using a submersible pump positioned 1 meter below the water's surface. Samples were collected by filtering a known volume of water through a glass-fiber filter (1.0 μm pore size) at a pressure of 10 mmHg. For turbid water (> 20 NTU), 200 mL was filtered while 500mL of water was filtered when turbidity was < 20 NTU to prevent clogging.

Filters were immediately frozen and transported to DWR's Bryte Laboratory for analysis using spectrophotometry in accordance with the Standard Method 10200 H (APHA, 2012). Samples were processed by mechanically grinding the filter and extracting phytopigments using acetone. Pigment absorption spectra were measured before and after acidification to quantify the amount of chlorophyll a and pheophytin a, respectively. Concentrations were calculated according to a formula specified in the methodology (APHA, 2012). Average analyte concentrations were then calculated per month, per region, and were normalized to the number of stations.

5.1.3 Results

5.1.3.1 Phytoplankton Identification

All organisms collected in 2020 fell into these ten algal groups:

- Pennate diatoms
- Centric diatoms
- Chrysophytes
- Synurophytes
- Cyanobacteria
- Cryptophytes
- Dinoflagellates
- Euglenoids
- Haptophytes
- Green Algae

The 10 most common genera collected in 2020 were, in order:

- Eucapsis (cyanobacterium)
- Chroococcus (cyanobacterium)
- Cyclotella (centric diatom)
- Chlorella (green alga)
- Plagioselmis (cryptophyte flagellate)
- Aulacoseira (centric diatom)
- Skeletonema (centric diatom)
- Cocconeis (pennate diatom)
- Nitzschia (pennate diatom)
- Pseudanabaena (cyanobacterium)

Of the ten groups identified, cyanobacteria constituted the vast majority (98.2%) of the organisms collected.

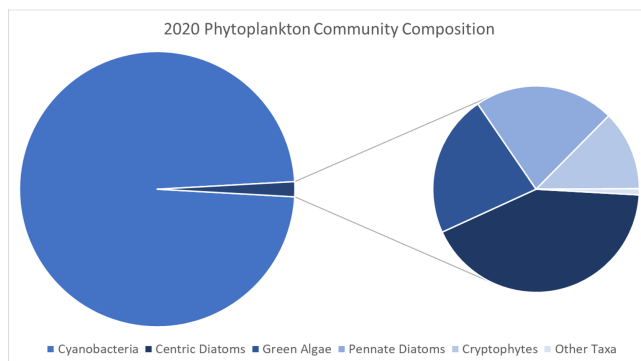


Figure 5.2: Phytoplankton composition by algal group (other are chrysophytes, ciliates, dinoflagellates, euglenoids, and haptophytes)

5.1.3.2 Pigment Concentrations

Some stations showed seasonal patterns in chlorophyll a concentration, while others did not. Most maxima occurred in spring and summer, while minima occurred in fall or winter. Monthly chlorophyll a concentrations throughout much of the estuary were low relative to historic levels. Of the 223 samples taken in 2020, 97.3% (217 samples) had chlorophyll a levels below 10 ug/L. Chlorophyll a levels below 10 ug/L are considered limiting for zooplankton growth (Müller-Solger et al., 2002). Of the 6 samples with chlorophyll a concentrations equal to or above 10 ug/L, five were at C10A (June through October) and one was at P8 in August.

The mean chlorophyll a concentration for all samples in 2020 was 2.86 ug/L; the median value was 1.88 ug/L. Both values are slightly higher than in 2019 (mean = 2.26 ug/L, median = 1.67 ug/L). The maximum chlorophyll a concentration in 2020 was 32.50 ug/L, recorded in July at C10A. This is similar to the 2019 maximum (38.10 ug/L). The minimum for 2020 chlorophyll a concentration was 0.53 ug/L, recorded at NZ325 in March, and again at C10A in November. It was nearly identical to the 2019 value (0.55 ug/L). Eight chlorophyll a samples were below the reporting limit.

The mean pheophytin a concentration for all samples in 2020 was 1.65 ug/L, slightly higher than the 2019 value (1.41 ug/L). The median value was 1.16 ug/L, which was also slightly higher than in 2019 (1.02 ug/L). The maximum pheophytin a concentration was 11.69 ug/L, recorded at NZ032 in August. This value was lower than in 2019 (13.55 ug/L). The minimum pheophytin a concentration was 0.50 ug/L, which is equivalent to the reporting limit; this was recorded at 2 stations (NZ002 and NZ004) in February. Twenty pheophytin a samples were below the reporting limit; they were observed primarily in the fall/winter.

5.1.3.3 Northern Interior Delta

Chlorophyll a average concentrations were higher in early winter, summer, and fall. The highest concentration was recorded at NZ068 in October (2.78 ug/L) and the lowest was recorded at C3A in December (0.53 ug/L), which was one of two recordings of the lowest concentration. The mean and median values were 1.42 ug/L and 1.18 ug/L, respectively. There were no samples below the detection limit.

Pheophytin a average concentrations were highest in the fall; values were similar to chlorophyll a. The maximum (3.20 ug/L) was recorded at NZ068 in September and the minimum (0.52 ug/L) was recorded at C3A in December, although there were four samples below the detection limit (C3A in November, and NZ068 in February, March, and July). The mean and median were 0.98 ug/L and 0.81 ug/L, respectively.

Phytoplankton average densities were highest in early winter and early fall, with cyanobacteria dominating throughout the year (“other taxa” are cryptophytes and dinoflagellates). Pennate diatom density was high in January, and green algae concentrations were relatively high in March and October.

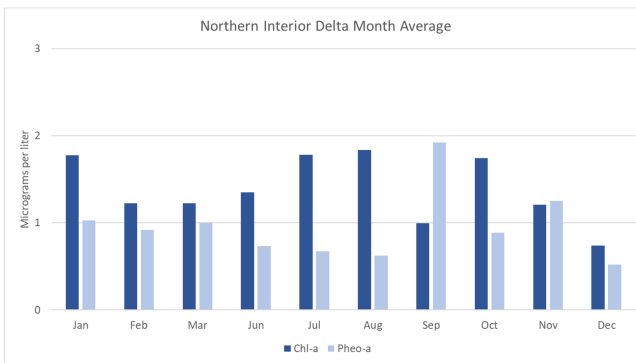


Figure 5.3: Average chlorophyll a and pheophytin a concentrations in the Northern Interior Delta

5.1.3.4 Southern Interior Delta

Chlorophyll a average concentrations were highest in the summer. The maximum was recorded at C10A in July (32.50 ug/L), which also was the maximum for the year; the minimum was at P8 in January (0.64 ug/L). The mean and median were 5.56 ug/L and 2.98 ug/L, respectively. There were two samples below the detection limit at C9 in December and MD10A in January.

Pheophytin a average concentrations were fairly constant throughout the year, with slight spikes in the summer months. The maximum pheophytin a value

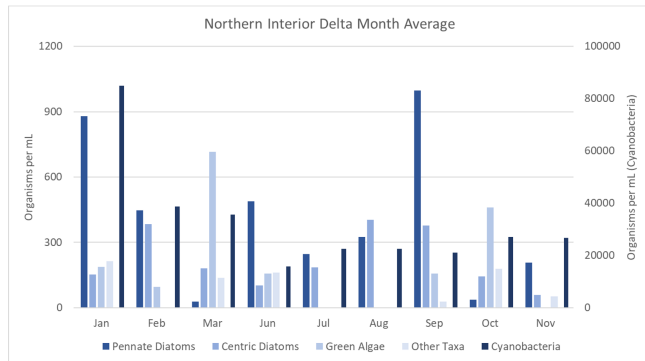


Figure 5.4: Average organism density in the Northern Interior Delta; other are chrysophytes, cryptophytes, and dinoflagellates

was recorded at C10A in July (6.06 ug/L); the minimum occurred at P8 in March (0.56 ug/L). The mean and median values were 1.84 ug/L and 1.46 ug/L, respectively. Two samples in January at MD10A and P8 were below the detection limit.

Phytoplankton average densities were highest in the summer and fall, with the highest concentrations occurring in July; “other taxa” are chrysophytes, cryptophytes, euglenoids, and synurophytes). Cyanobacteria dominated throughout the year and centric diatom concentrations were relatively high in the summer months.

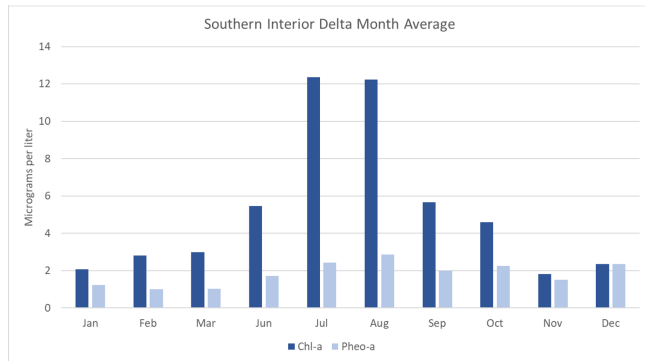


Figure 5.5: Average chlorophyll a and pheophytin a concentrations in the Southern Interior Delta

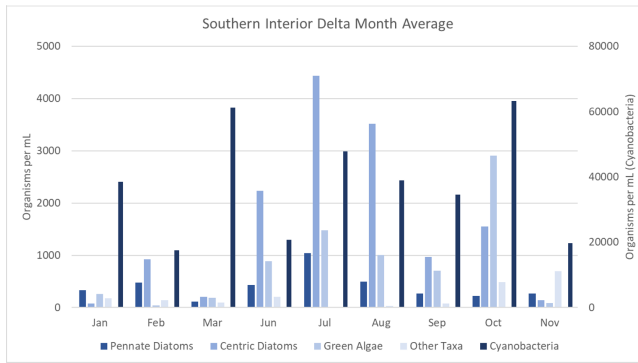


Figure 5.6: Average organism density in the Southern Interior Delta; other are chrysophytes, cryptophytes, and dinoflagellates

5.1.3.5 Central Delta

Chlorophyll a average concentrations were highest in the summer and early fall months. The highest chlorophyll a concentration for this region at occurred at D16 in September (8.50 ug/L); the minimum occurred at the same station in January (1.01 ug/L). The mean and median values were 2.63 ug/L and 2.09 ug/L, respectively. There were no samples below the detection limit.

Pheophytin a average concentrations were relatively consistent throughout the year excluding a large spike in November, when the highest concentration in the region was recorded (15.40 ug/L, station D19). The minimum occurred at D19 in October (0.50 ug/L). The mean and median values were 1.28 ug/L and 0.90 ug/L, respectively. There was one sample below the detection limit at D16 in January.

With the exception of cyanobacteria, phytoplankton average densities were low all year except for a bloom of centric diatoms in August (“other taxa” are chrysophytes, cryptophytes, and green algae).

5.1.3.6 Confluence

Chlorophyll a average concentrations were highest during early spring and mid-summer. The highest concentration occurred at D12 in August (5.27 ug/L); the minimum was recorded at D22 in November (0.95 ug/L). The mean and median values were 2.53 ug/L and 2.12 ug/L, respectively. There was one sample below the detection limit at D10 in October.

Pheophytin a average concentrations were relatively consistent throughout the year except for a peak in September, which was the maximum for the year. The maximum concentration was recorded at D22 in September (5.20 ug/L) and the minimum at the same station in January (0.51 ug/L). The mean and median for

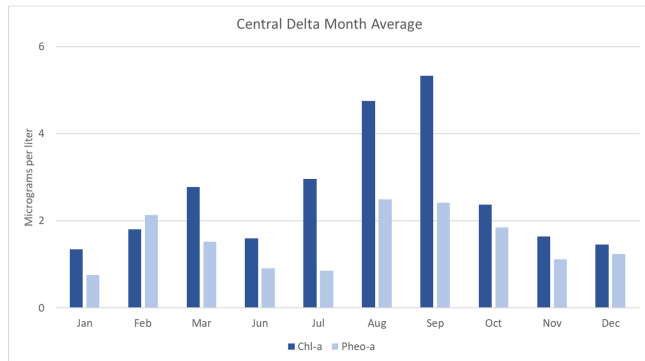


Figure 5.7: Average chlorophyll a and pheophytin a concentrations in the Central Delta

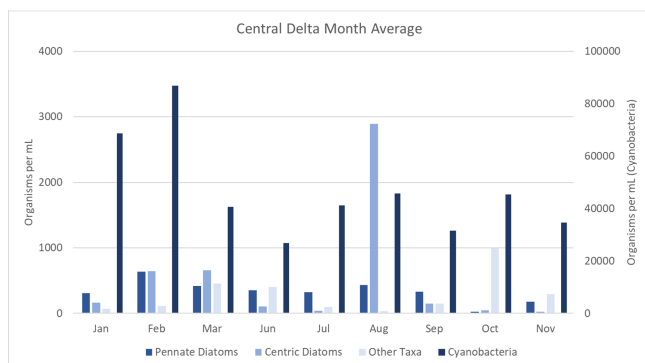


Figure 5.8: Average organism density in the Central Delta; other are chrysophytes, cryptophytes, and dinoflagellates

this region were 1.47 ug/L and 1.24 ug/L, respectively. There were two samples below the detection limit at D10 in August and D22 in February.

Phytoplankton average densities were higher in winter and early spring; the peak of “other taxa” in October was mainly cryptophytes and green algae; “other taxa” are chrysophytes, cryptophytes, euglenoids, and green algae). Cyanobacteria also dominated throughout the year.

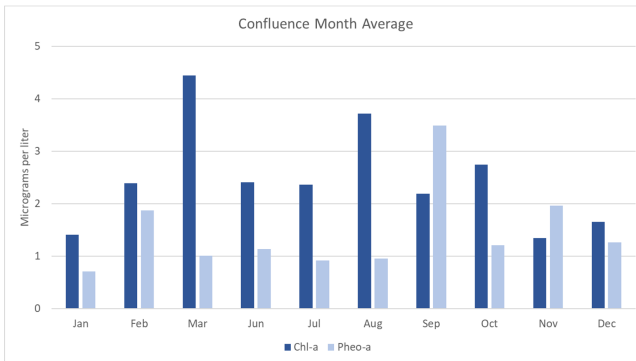


Figure 5.9: Average chlorophyll a and pheophytin a concentrations in the Confluence

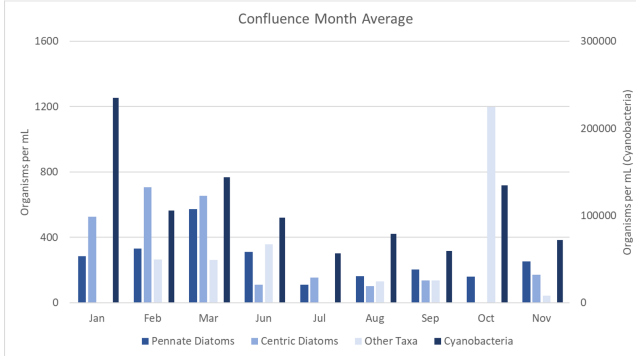


Figure 5.10: Average organism density in the Confluence; other are chrysophytes, cryptophytes, and dinoflagellates

5.1.3.7 Grizzly Bay and Suisun Bay

Chlorophyll a average concentrations in this region was relatively consistent throughout the year. The maximum was recorded at NZS42 in August (9.69 ug/L); the minimum was recorded at D7 in January (0.67 ug/L). The mean and median were 2.71 ug/L and 2.05 ug/L, respectively. There were two samples below the detection limit at D7 in August and NZS42 in September.

Pheophytin a average concentrations were relatively consistent throughout the year except for a peak in August, which was the maximum for the year. The maximum concentration was recorded at NZ032 in August (11.69 ug/L) and the minimum at D8 in July (0.56 ug/L). The mean and median were 1.39 ug/L and 1.00 ug/L, respectively. There were two samples below the detection limit at D7 in February and D8 in August.

Phytoplankton average densities were relatively higher early in the year, driven mostly by pennate diatoms, centric diatoms, and cyanobacteria (“other taxa” are cryptophytes, dinoflagellates, euglenoids, green algae, and haptophytes). The peak of “other taxa” in October was driven mainly by cryptophytes and green algae. Except for cyanobacteria, average densities were low compared to other regions (less than 1000 organisms per milliliter)

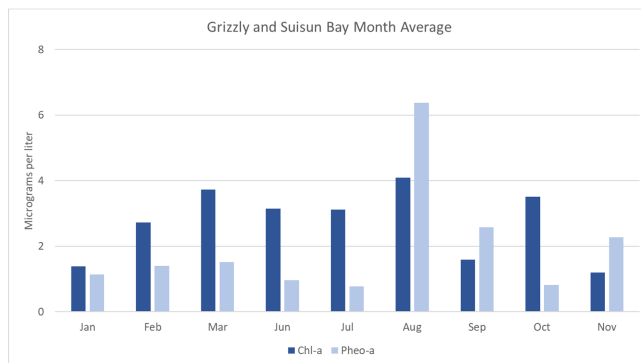


Figure 5.11: Average chlorophyll a and pheophytin a concentrations in the Grizzly/Suisun Bays

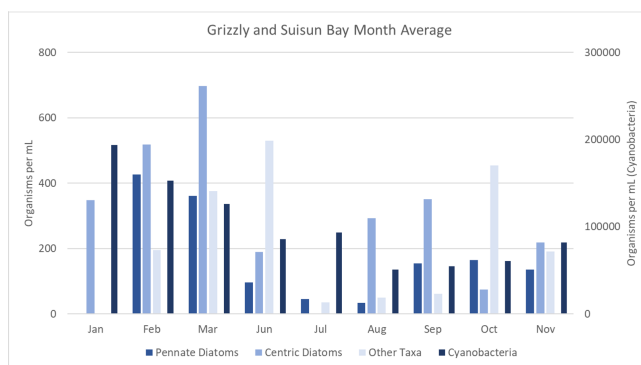


Figure 5.12: Average organism density in the Grizzly/Suisun Bays; other are chrysophytes, cryptophytes, and dinoflagellates

5.1.3.8 San Pablo Bay

Chlorophyll a average concentrations were slightly higher in summer and early fall. The maximum was recorded at D41A in September (8.93 ug/L); the minimum concentration was recorded at NZ325 in March, one of two minimums recorded for the year (0.53 ug/L). The mean and median were 2.02 ug/L and 1.71 ug/L, respectively. There were three samples below the detection limit: D6 and NZ325 in August, and NZ002 in November.

Pheophytin a average concentrations were lower in the first half of the year, and higher in the second half. The maximum was recorded at D41A in October (7.72 ug/L) and the minimum at both NZ002 and NZ004 in February, which were the lowest values for the year and also the detection limit (0.50 ug/L). The mean and median were 1.76 ug/L and 0.99 ug/L, respectively. There were nine samples below the detection limit: D41, D41A, and NZ325 in January; D41 and NZ325 in February; NZ325 in March; NZ004 in June and July; and NZ325 in October.

There were peaks of cyanobacteria in January and October; most of the phytoplankton average densities were lower for the rest of the year (“other taxa” are cryptophytes, euglenoids, green algae, and haptophytes). The peak of “other taxa” in June was driven by cryptophytes and green algae.

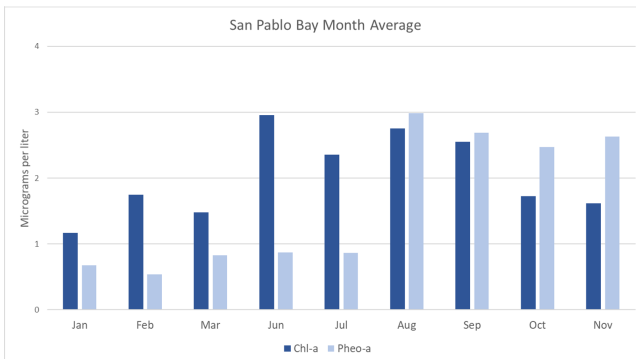


Figure 5.13: Average chlorophyll a and pheophytin a concentrations in the San Pablo Bay

5.1.4 References

[APHA] American Public Health Association, American Waterworks, and Water Environmental Federation. 2012. Standard Methods for the Examination of

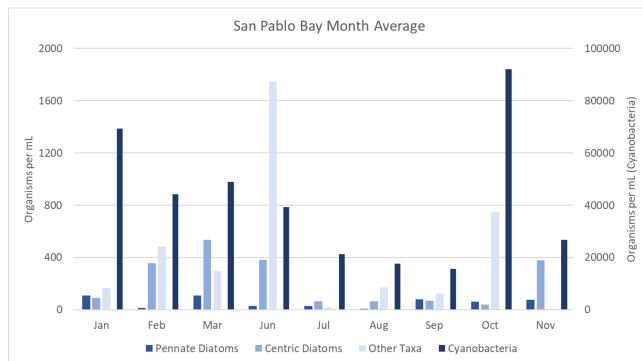


Figure 5.14: Average organism density in the San Pablo Bay; other are chrysophytes, cryptophytes, and dinoflagellates

Water and Wastewater. 22nd ed. Washington, D.C.: American Public Health Association.

Alpine, A. E., and Cloern, J. E. 1992. Trophic interactions and direct physical effects control phytoplankton biomass and production in an estuary. Limnol. Oceanogr. 37: 946-955

Carmichael, W., ed. 1981. The Water Environment, Algal Toxins and Health. Plenum Press, New York, N. Y.

Gannon, J. E. and R. S. Stemberger. 1978. Zooplankton (especially crustaceans and rotifers) as indicators of water quality. Trans. Amer. Microsc. 97:16.

Horne, A. and Goldman, C. 1994. Limnology. 2nd ed. New York, New York, McGraw-Hill, Inc.

Müller-Solger AB, Jassby AD, Müller-Navarra DC. 2002. Nutritional quality of food resources for zooplankton (*Daphnia*) in a tidal freshwater system (Sacramento-San Joaquin River Delta). Limnology and Oceanography 47(5): 1468-1476.

Utermöhl, H. 1958. Zur Vervollkommnung der quantitativen Phytoplankton Methodik. Mitt. Int. Verh. Limnol. 9: 38.

van den Hoek, C., D.G. Mann, and H.M. Jahns. 1995. Algae: an introduction to Phycology. Cambridge University Press, United Kingdom.

5.2 Contact Info

For questions related to EMP's phytoplankton data sets, please contact Tiffany Brown at tiffany.brown@water.ca.gov.

Chapter 6

Zooplankton

Background

Zooplankton are a vital trophic link between aquatic primary producers and higher-level consumers of the San Francisco Estuary (SFE). As primary consumers of phytoplankton, zooplankton facilitate the flow of carbon into a large and complex food web, historically supporting abundant fisheries in the region (Schroeter et al. 2015; Kimmerer et al. 2018). Many fishes, including Striped Bass (*Morone saxatilis*) and Chinook Salmon (*Oncorhynchus tshawytscha*) feed on zooplankton while rearing in the estuary as larvae and juveniles (Goertler et al. 2018; Heubach et al. 1963), while others like Tule Perch (*Hysterocarpus traski*) and Prickly Sculpin (*Cottus asper*) feed on zooplankton throughout their lifetimes (Kimmerer 2006Feyrer et al. 2003)). Zooplankton in the SFE are also a key food source for several endangered and threatened species, notably the Delta Smelt (*Hypomesus transspacificus*) and Longfin Smelt (*Spirinchus thaleichthys*) (Hobbs et al. 2006; Slater and Baxter 2014).

This importance of zooplankton prompted the implementation of the Zooplankton Study in 1972 to assess fish food resources in the upper SFE. Mandated by the State Water Resources Control Board's Water Right Decision D-1641, the study is conducted jointly by the California Department of Fish and Wildlife and the California Department of Water Resources under the guidance and management of the Interagency Ecological Program. For nearly 5 decades, this study has monitored the zooplankton community in the region, tracking abundance trends and distributional patterns, detecting and monitoring introduced species, and documenting the dramatic shifts in the community's composition. Changes in zooplankton abundance and composition have since been linked to major declines of the pelagic fishes in the upper estuary (Sommer et al. 2007; Winder and Jassby 2011).

Methods

Zooplankton sampling has been conducted since 1974 at least once a month March–November through 1995, monthly from 1995 on, at 20 fixed stations in the upper SFE (Figure 6.1). Three gear types are used for each sampling event: a pump with a 43-micron mesh net for micro-zooplankton (rotifers, nauplii, and small cyclopoid copepods); a Clarke-Bumpus (CB) net with a 160-micron mesh for sampling meso-zooplankton (cladocera and most juvenile and adult calanoid copepods); and a mysid net with a 505-micron mesh for sampling mysid shrimp and other macro-zooplankton. Both the mysid and CB nets are attached to a sled and towed obliquely from the bottom through the surface for a 10-minute tow. Volume is measured using a General Oceanics flowmeter placed in the mouth of each net so that: $V=(\text{end meter}-\text{start meter})k^*a$; where V is the volume of water sampled, k is a flowmeter correction value, and a is the area of the mouth of the net. The Teel Marine 12V utility pump is also used at each station to sample approximately 19.8 gallons from the entire water column, which is filtered through a 43-micron mesh net to concentrate the pump sample. Samples are preserved in 10% formalin with Rose Bengal dye before being processed in the laboratory for identification and enumeration of organisms using a dissecting microscope. More information about the sampling and processing methods can be found in the metadata at [here](#) (link currently broken).

Abundance indices are calculated for each organism based on the gear type most effective at its capture and reported as the mean catch-per-unit-effort (CPUE). CPUE is calculated as the number of each organism collected per cubic meter of water sampled, so that: $\text{CPUE}=s^*V^{-1}$; where s is the estimated count of the target organism in the sample. Copepod abundance indices reported here only include adults, as juveniles were not always identified to species. Annual and seasonal abundance indices were calculated using 14 fixed stations sampled consistently since 1974 (Figure 6.1) and 2 non-fixed stations sampled where bottom specific conductance was roughly 2 and 6 millisiemens per centimeter (approximately 1 and 3 psu).

To analyze long-term trends (1974 to present), annual abundance indices were calculated as the mean CPUE for samples collected from March through November, as winter sampling was inconsistent before 1995. Seasonal abundance indices were calculated as the mean CPUE for samples collected during each season: winter (previous December to February), spring (March to May), summer (June to August), and fall (September to November). Long-term seasonal trends for winter are only shown for 1995 to present. Spatial distribution indices for organisms is described as seasonal mean CPUE for by region. Estuary regions were defined as San Pablo Bay (stations D41 and D41A), Suisun Bay (stations D6, 28, 54, and 48), Suisun Marsh (stations 32 and S42), West Delta (stations 60, 64, and 74), Central Delta (stations D16, 86, and D28), and the East Delta (92 and M10).

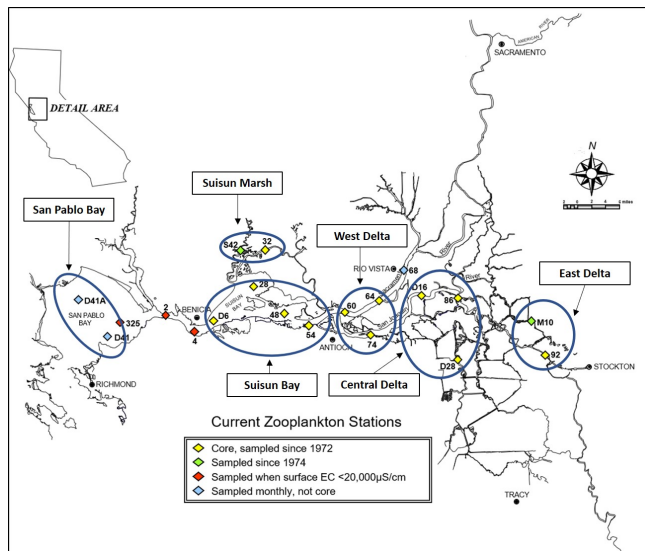


Figure 6.1: Map of fixed Zooplankton Study stations in the San Francisco Estuary.

6.1 Current Report

6.1.1 Introduction

This report presents zooplankton annual and seasonal abundance indices and distribution trends from 1974 through 2020 for the most common copepods, cladocera, rotifers, and mysids of the upper estuary.

6.1.2 Trends

Since the implementation of the Zooplankton Study in 1974, a significant decrease in the overall abundance of zooplankton has been detected in the estuary (Figure 70). Only the abundance of cyclopoid copepods increased in the region during this period, driven by the invasion and spread of *Limnoithona tetraspina*. The overall decrease in zooplankton abundance in the estuary can be attributed to a series of invasions into the estuary, most notably that of the Asian clam *Potamocorbula amurensis* in the mid-1980s (Kimmerer, Gartside, and Orsi 1994; Carlton et al. 1990). The spread of *P. amurensis* throughout SFE has had significant impacts on planktonic abundance in the upper estuary due to its high filtration feeding rates on phytoplankton and copepod nauplii. Not only has

abundance decreased for most of the zooplankton groups, but dramatic shifts in the composition of these communities have been detected during the study period. These changes have been driven by the introduction and spread of non-native zooplankton species throughout the estuary, compounded with changes to the abiotic and biotic environments.

6.1.2.1 Calanoid copepods

While overall calanoid copepod abundance has declined slightly over the study period, community composition has shifted dramatically (Figure 70A). When the study began in the early 1970s the copepods *Eurytemora affinis* and *Acartia* spp. dominated the calanoid community. The non-native *E. affinis* was once the primary prey item of the endangered Delta Smelt, but its abundance has declined to a fraction of what it once was, forcing fish to prey switch to more recently introduced calanoids like *Pseudodiaptomus forbesi* (Moyle et al. 1992; Slater and Baxter 2014). One of the first recorded introduced calanoid copepods was *Sinocalanus doerrii*, a freshwater species native to China that invaded the estuary in 1978 and became the most dominant calanoid species in the estuary for a decade (Orsi et al. 1983). Then in 1987, after the invasion of *P. amurensis*, the calanoid *Pseudodiaptomus forbesi* was introduced and first detected in the region, competing with the abundant *E. affinis* (Orsi and Walter 1991). *P. forbesi* quickly became the numerically dominant calanoid in the upper estuary and remains the most abundant to this day. Another introduction occurred in 1993, when the predatory calanoid copepod *Acartiella sinensis* quickly became the second most abundant calanoid in the upper estuary, dominating the low-salinity zone in Suisun and the West Delta (Orsi and Ohtsuka 1999). This invasion was hypothesized to have narrowed the range of *P. forbesi* and calanoid copepods towards the freshwater zone of the estuary (Figure 71A), as predation on *P. forbesi* nauplii by *A. sinensis* has been recorded (Kayfetz and Kimmerer 2017).

In general, calanoid copepod abundance is highest in the estuary during the summer and fall months, with lowest abundances during the winter (Figure 72A). While calanoid copepod abundance peaked in the summer of 2017 at a nearly 20 year high, 2018 through 2020 abundance returned to levels comparable to the previous two decades. In 2020 the distribution of calanoids throughout the estuary was similar to the last two years, with *P. forbesi* the most abundant in summer and fall in most of the upper estuary (Figure 72A). The predatory *Acartiella sinensis* was seen in highest densities in the summer and fall mostly in the Suisun Marsh and Suisun Bay regions, similar to 2018 and 2019. In fall 2020, *A. sinensis* was the most abundant calanoid in Suisun, where it co-occurred with high densities of one of its primary prey items *Limnoithona tetraspina* (Figure 72B), while *P. forbesi* was most abundant to the east of Suisun Bay. *Acartia* spp. was the only native calanoid copepod commonly found in 2020, but it was restricted to Suisun Bay and San Pablo Bay in the lower reaches of the estuary. *Eurytemora affinis* was most dominant calanoid upriver of Suisun Bay estuary

in the spring of 2020, similar to seasonal distribution patterns of the last two decades.

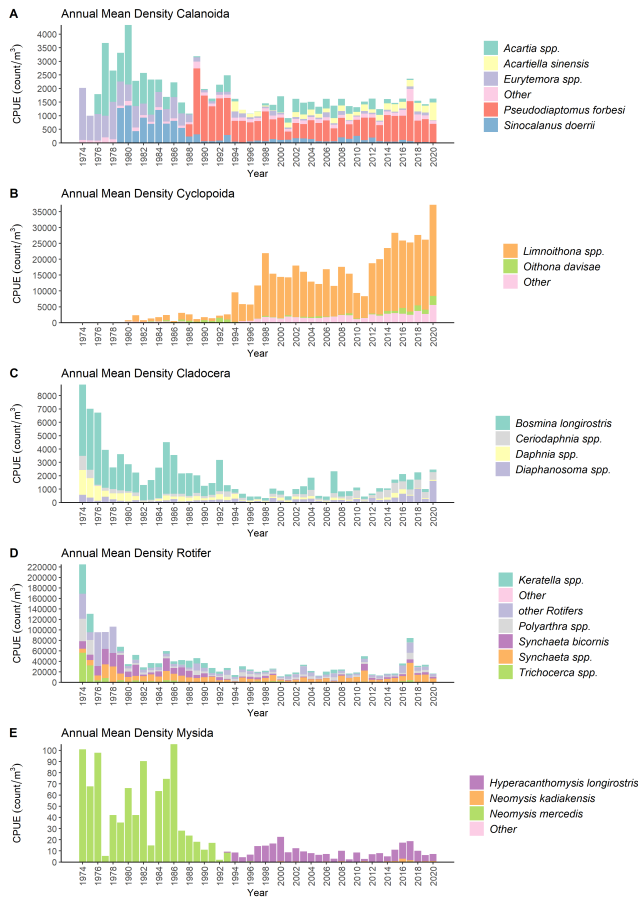


Figure 6.2: Annual (Mar-Nov) mean zooplankton CPUE for A) Calanoid CPUE in the CB net, B) Cyclopoida CPUE in pump samples, C) Cladocera CPUE in the CB net, D) Rotifer CPUE in pump samples, and E) Mysid CPUE in the mysid net.

6.1.2.2 Cyclopoid copepods

While overall zooplankton abundance has declined over the study period, the abundance of cyclopoid copepods exploded (Figure 70B). The native *Oithona* spp. and *Acanthocyclops* copepods were at low abundances when the study began, but with the introduction of *Limnoithona sinensis* in the early 1980s, and the later identification of the invasive *Limnoithona tetraspina* in 1993, cyclopoid

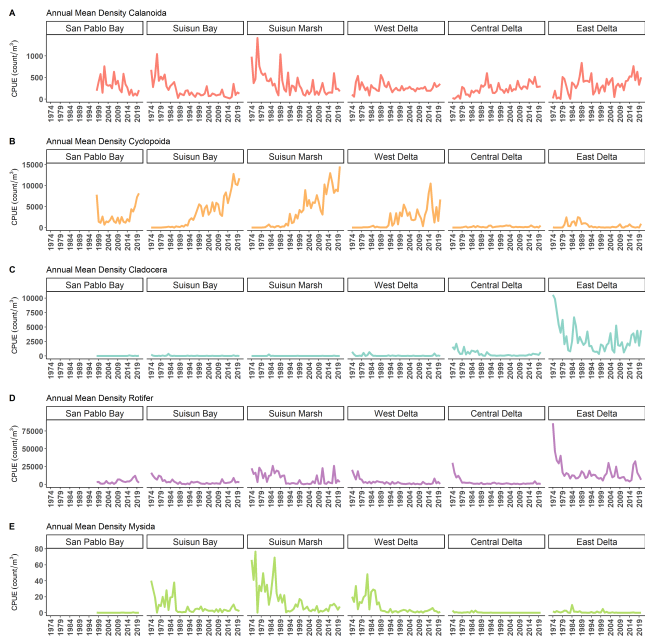


Figure 6.3: Annual (Mar-Nov) mean zooplankton CPUE by region and order for A) Calanoida CPUE in the CB net, B) Cyclopoda CPUE in pump samples, C) Cladocera CPUE in the CB net, and D) Mysid CPUE in the mysid net, from the EMP survey.

indices have increased dramatically (Ferrari and Orsi 1984; Orsi and Ohtsuka 1999). Abundance indices for the two species of *Limnoithona* were reported together from 1980 through 2006 as *Limnoithona* spp., then separately since 2007 when they were identified and enumerated as *L. sinensis* and *L. tetraspina*. In 2020, *L. tetraspina* abundance was the highest observed for all copepods (Figure 70B).

Much smaller than calanoid copepods collected in the CB net, the *Limnoithona* cyclopoids are best retained in pump samples, which use a smaller mesh. Since the early 1990s, *Limnoithona* spp. abundance has been higher than calanoid copepod abundance, and the small *L. tetraspina* has become the most common zooplankton in the upper estuary. This increase in *L. tetraspina* abundance is likely due to a decline of Northern Anchovy in the upper SFE and subsequent decreased predation (Kimmerer 2006), as well as the cyclopoid's small size, high growth rate, and motionless behavior, making it very difficult for visual feeders to capture (Bouley and Kimmerer 2006; Greene et al. 2011). These characteristics may increase its ability to escape predation in a region where visual predation is most dominant among fish (Kimmerer 2006). The introduction of *L. tetraspina* is also linked to the reduction of the range of *P. forbesi* out of the low-salinity zone of the estuary, as high *L. tetraspina* densities may have fed and sustained larger populations of the predatory *A. sinensis*, which also fed on *P. forbesi* nauplii (Kayfetz and Kimmerer 2017).

Seasonally, *Limnoithona tetraspina* peaks in summer and fall (Figure 71B), with lower abundance in winter and spring. As in prior years, this cyclopoid was most abundant in the low-salinity zone of the estuary in Suisun Bay and the West Delta (Figure 72B). *Oithona davisae*, a native cyclopoid, was the most abundant cyclopoid in the higher-salinity San Pablo Bay in summer and fall (Figure 72B).

6.1.2.3 Cladocera

The cladoceran community of the upper estuary is composed of *Bosmina*, *Daphnia*, *Ceriodaphnia*, and *Diaphanosoma* species, whose populations have also substantially declined since the onset of the study (Figure 70C). These cladocera tend to be herbivorous, feeding primarily on phytoplankton, and were likely hard hit by the invasion of *P. amurensis* (Baxter et al. 2008; Kratina and Winder 2015). Cladocerans make up a significant portion in the diets of Delta Smelt, juvenile Chinook Salmon, and young-of-the-year Striped Bass throughout the upper estuary (Heubach et al. 1963; Slater and Baxter 2014; Goertler et al. 2018). The invasion and increase of available copepod prey such as *P. forbesi* and the decline in cladocera has created a shift in the nutritional content of the plankton community available for fish, with yet to be determined consequences (Kratina and Winder 2015).

While Cladocera abundance has declined overall since the study began, recent years abundance has been increased and in 2020 cladocera abundance was the highest observed since 1992 (Figure 71C). In the high outflow year of 2017 some

cladocera, namely Bosmina, were found downstream in Suisun and the West Delta, while in 2020 the highest densities of cladocera were found in the East Delta, with trace concentrations found in other regions of the estuary (Figure 72C).

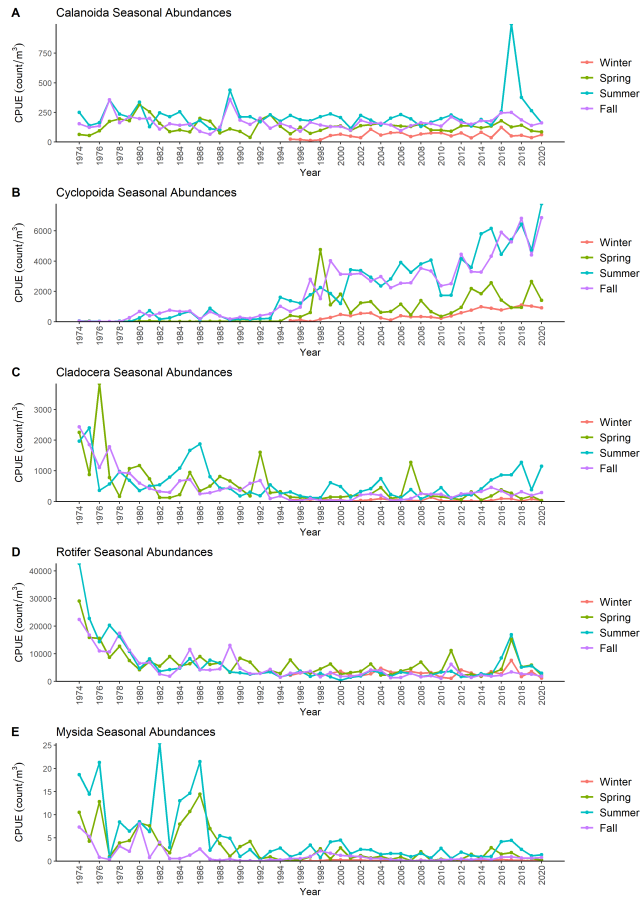


Figure 6.4: Seasonal mean zooplankton CPUE. Spring, summer, and fall are reported for 1974-2018, winter is reported for 1995-2019. A) Calanoid CPUE in the CB net. B) Cyclopoida CPUE in pump samples. C) Cladocera CPUE in the CB net. D) Rotifer CPUE in pump samples. E) Mysid CPUE in the mysid net

6.1.2.4 Rotifer

While they are the most abundant zooplankton in the estuary, long-term sampling of rotifers using the pump system shows a dramatic decrease in their annual abundance in the estuary since the beginning of this study (Figure 70D).

Several species of rotifers make up the community: most abundant being the Polyarthra, Synchaeta, and Keratella genera. Interestingly, the decline of rotifer abundance beginning in the late 1970s preceded the invasion of *P. amurensis* in the estuary (Cloern and Jassby 2012).

The distribution and abundance of rotifers were similar in 2020 to previous years, with abundances similar to those found since the invasion of *P. amurensis*. Overall rotifer abundance peaked in the summer and spring (Figure 71D). Keratella and Polyarthra tend to be most abundant in the freshwater and low-salinity zone of the estuary, while Synchaeta species occur most in the higher-salinity areas of San Pablo Bay and Suisun (Figures 3D and 4D)(Winder and Jassby 2011). A spatial and temporal split was discernable between Synchaeta and other rotifers, with Synchaeta having highest densities in the low-salinity zone Bay during the spring, and other rotifers being most abundant in the East Delta in summer.

6.1.2.5 Mysida

Not only have mysid abundances declined significantly since the 1970s, but the community has also shifted from being composed almost entirely by the native *Neomysis mercedis*, to being dominated by the non-native *Hyperacanthomysis longirostris* (formerly *Acanthomysis bowmani*) (Figure 70E). The first significant decline in *N. mercedis* occurred during the 1976-1977 drought, likely caused by food limitation from an absence of diatoms due to very low river discharges (Siegfried et al. 1979; Cloern et al. 1983). The populations of *N. mercedis* were able to rebound after the years of drought and stayed at high densities in the Suisun Bay region of the upper estuary until the introduction of *P. amurensis* in the mid-1980s, after which their numbers crashed.

In 1993 the introduced *H. longirostris* was first detected by this study, shortly after the decline of *N. mercedis*, and it quickly became the most common mysid in the system. However, overall mysid abundances have not returned to their pre-clam invasion levels (Modlin and Orsi 1997, Figure 70E). Mysids have always peaked in the spring and summer months, fluctuating with the higher productivity in the estuary during those seasons (Figure 71E). Historically mysids have been of critical importance in the diets of many fish species in the SFE including Delta Smelt, Longfin Smelt, Striped Bass, and Chinook Salmon (Moyle et al. 1992; Feyrer et al. 2003; CDFG 2009; Goertler et al. 2018). However, the decline of mysids in the upper estuary has resulted in a significant decrease in their presence in the diets of fishes of the region (Feyrer et al. 2003). This general decline in abundance continued in 2019, even though 2016 and 2017 had a modest peak in mysid abundances (Figure 70E), and the distribution and timing of peaks stayed similar over the last two decades (Hennessy 2018). *Hyperacanthomysis longirostris* was again the most common mysid in the estuary during all seasons, while the once common and native *Neomysis mercedis* continued to be almost imperceptible in the region. This has been the overall trend in

the estuary's mysid communities since 1994. As in prior years, mysids in 2019 were most abundant during the summer and fall (Figure 71E), and highest concentrations occurred in the low-salinity zone of Suisun Bay and Marsh (Figure 72E).

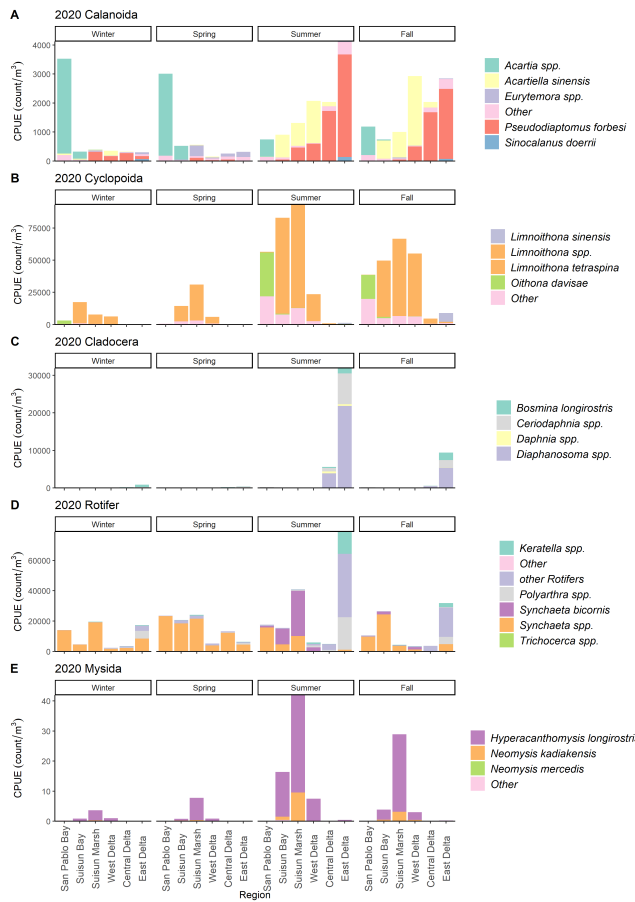


Figure 6.5: Seasonal mean zooplankton CPUE for reporting year by region for A) Calanoid CPUE in the CB net, B) Cyclopoida CPUE in pump samples, C) Cladocera CPUE in the CB net, D) Rotifer CPUE in pump samples, and E) Mysid CPUE in the mysid net.

6.1.3 Conclusion

In 2019 the Zooplankton Study recorded the abundances of calanoids, cladocera, rotifers, and mysids at lower densities comparable to other recent years

and consistent with the downward historic trends in the estuary. Calanoid and cyclopoid copepod abundance peaked in fall, whereas cladocera, rotifers, and mysids peaked in summer. The small, abundant *Limnoithona tetraspina* was again the most abundant copepod in the upper estuary. This multi-decade zooplankton study has enabled researchers and managers to track the shifts in zooplankton abundances and community composition across the estuary for nearly 5 decades. The Zooplankton Study has documented the introduction and dominance of *Pseudodiaptomus forbesi*, *Limnoithona tetraspina*, and *Hypercanthomysis longirostris*, as well as the community's response to the invasive clam *Potamocorbula amurensis*. Understanding these dynamics and how they have fundamentally changed trophic interactions is critical to assessing food resources for fish and conservation strategies in the San Francisco Estuary.

6.1.4 References

- Baxter R, Feyrer F, Nobriga M, Sommer T. 2008. Pelagic Organism Decline Progress Report: 2007 Synthesis of Results. Bouley P, Kimmerer WJ. 2006. Ecology of a highly abundant, introduced cyclopoid copepod in a temperate estuary. *Mar Ecol Prog Ser*. 324(October):219–228.
- Carlton JT, Thompson JK, Schemel LE, Nichols FH. 1990. Remarkable invasion of San Francisco Bay (California, USA) by the Asian clam *Potamocorbula amurensis*. I. Introduction and dispersal. *Mar Ecol Prog Ser*. 66:81–94.
- CDFG. 2009. A Status Review of the Longfin Smelt (*Spirinchus thaleichthys*) in California. Sacramento.
- Cloern JE, Alpine AE, Cole BE, Wong RLJ, Arthur JF, Ball MD. 1983. River discharge controls phytoplankton dynamics in the northern San Francisco Bay estuary. *Estuar Coast Shelf Sci*. 16(4):415–429.
- Cloern JE, Jassby AD. 2012. Drivers of change in estuarine-coastal ecosystems: Discoveries from four decades of study in San Francisco Bay. *Rev Geophys*. 50:4001.
- Ferrari FD, Orsi J. 1984. *Oithona daviseae*, new species, and *Limnoithona sinensis* (Burckhardt, 1912) (Copepoda: Oithonidae) from the Sacramento-San Joaquin Estuary, California. *J Crustac Biol*. 4(1):106–126.
- Feyrer F, Herbold B, Matern SA, Moyle PB. 2003. Dietary shifts in a stressed fish assemblage: Consequences of a bivalve invasion in the San Francisco Estuary. Goertler P, Jones K, Cordell J, Schreier B, Sommer T. 2018. Effects of extreme hydrologic regimes on juvenile Chinook Salmon prey resources and diet composition in a large river floodplain. *Trans Am Fish Soc*. 147:287–299.

- Greene VE, Sullivan LJ, Thompson JK, Kimmerer WJ. 2011. Grazing impact of the invasive clam *Corbula amurensis* on the microplankton assemblage of the northern San Francisco estuary. *Mar Ecol Prog Ser.* 431(February):183–193.
- Hennessy A. 2018. Zooplankton Monitoring 2017. *Interag Ecol Progr News.* 32(1):21–32.
- Heubach W, Toth RJ, Mccready AM. 1963. Food of Young-of-the-year Striped Bass (*Roccus Saxatilis*) in the Sacramento-San Joaquin River. *Calif Fish Game.* 49(4):224–239.
- Hobbs JA, Bennett WA, Burton JE. 2006. Assessing nursery habitat quality for native smelts (Osmeridae) in the low-salinity zone of the San Francisco estuary. *J Fish Biol.* 69(3):907–922.
- Kayfetz K, Kimmerer W. 2017. Abiotic and biotic controls on the copepod *Pseudodiaptomus forbesi* in the upper San Francisco Estuary. *Mar Ecol Prog Ser.* 581(Runge 1988):85–101.
- Kimmerer W, Ignoffo TR, Bemowski B, Modéran J, Holmes A, Bergamaschi B. 2018. Zooplankton dynamics in the Cache Slough Complex of the upper San Francisco estuary. *San Fr Estuary Watershed Sci.* 16(3).
- Kimmerer WJ. 2006. Response of anchovies dampens effects of the invasive bivalve *Corbula amurensis* on the San Francisco Estuary foodweb. *Mar Ecol Prog Ser.* 324(Cloern 1982):207–218.
- Kimmerer WJ, Gartside E, Orsi JJ. 1994. Predation by an introduced clam as the likely cause of substantial declines in zooplankton of San Francisco Bay. *Mar Ecol Prog Ser.* 113(1–2):81–94.
- Kratina P, Winder M. 2015. Biotic invasions can alter nutritional composition of zooplankton communities. *Oikos.* 124:1337–1345.
- Modlin RF, Orsi JJ. 1997. *Acanthomysis bowmani*, a new species, and *A. aspera* Li, Mysidacea newly reported from the Sacramento-San Joaquin Estuary, California (Crustacea: Mysidae). *Proc Biol Soc Washingt.* 110(3):439–446.
- Moyle PB, Herbold B, Stevens DE, Miller LW. 1992. Life history and status of delta smelt in the Sacramento-San Joaquin estuary, California. *Trans Am Fish Soc.* 121(1):67–77.
- Orsi J, Walter TC. 1991. *Pseudodiaptomus forbesi* and *P. marinus* (Copepoda: Calanoida), the latest copepod immigrants to California's Sacramento-San Joaquin Estuary. *Bull Plankt Soc Japan.*:553–562.
- Orsi JJ, Bowman TE, Marelli DC, Hutchinson A. 1983. Recent introduction of the planktonic calanoid copepod *Sinocalanus doerrii* (Centropagidae) from mainland China to the Sacramento-San Joaquin Estuary of California. *J Plankton Res.* 5(3):357–375.
- Orsi JJ, Ohtsuka S. 1999. Introduction of the Asian copepods *Acartiella sinensis*, *Tortanus dextrilobatus* (Copepoda: Calanoida), and *Limnoithona tetraspina*

(Copepoda: Cyclopoida) to the San Francisco Estuary, California, USA. *Plankt Biol Ecol.* 46(2):128–131.

Schroeter RE, O'Rear TA, Young MJ, Moyle PB. 2015. The aquatic trophic ecology of Suisun Marsh, San Francisco Estuary, California, during autumn in a wet year. *San Fr Estuary Watershed Sci.* 13(3).

Siegfried CA, Kopache ME, Knight AW. 1979. The Distribution and Abundance of Neomysis mercedis in Relation to the Entrapment Zone in the Western Sacramento-San Joaquin Delta. *Trans Am Fish Soc.* 108(3):262–270.

Slater SB, Baxter R. 2014. Diet, Prey Selection, and Body Condition of Age-0 Delta Smelt, *Hypomesus transpacificus*, in the Upper San Francisco Estuary. *San Fr Estuary Watershed Sci.* 12(3):1–24.

Sommer T, Armor C, Baxter R, Breuer R, Brown L, Chotkowski M, Culberson S, Feyerer F, Gingras M, Herbold B, et al. 2007. The collapse of pelagic fishes in the upper San Francisco Estuary. *Fisheries.* 32(6):270–277.

Winder M, Jassby AD. 2011. Shifts in Zooplankton Community Structure: Implications for Food Web Processes in the Upper San Francisco Estuary. *Estuaries and Coasts.* 34:675–690.

6.2 Data and Contact Info

Data available on the Environmental Data Initiative portal or the CDFW FTP site.

For questions related to EMP's zooplankton data sets, please contact Arthur Barros at arthur.barros@wildlife.ca.gov.

Part III

Special Studies

Chapter 7

Coming Soon!

Check back later for updates on EMP's projects.